



Year: 2017

Postprandial macrophage-derived IL-1 stimulates insulin, and both synergistically promote glucose disposal and inflammation

Dror, Erez ; Dalmas, Elise ; Meier, Daniel T ; Wueest, Stephan ; Thévenet, Julien ; Thienel, Constanze ; Timper, Katharina ; Nordmann, Thierry M ; Traub, Shuyang ; Schulze, Friederike ; Item, Flurin ; Vallois, David ; Pattou, Francois ; Kerr-Conte, Julie ; Lavallard, Vanessa ; Berney, Thierry ; Thorens, Bernard ; Konrad, Daniel ; Böni-Schnetzler, Marianne ; Donath, Marc Y

Abstract: The deleterious effect of chronic activation of the IL-1 system on type 2 diabetes and other metabolic diseases is well documented. However, a possible physiological role for IL-1 in glucose metabolism has remained unexplored. Here we found that feeding induced a physiological increase in the number of peritoneal macrophages that secreted IL-1, in a glucose-dependent manner. Subsequently, IL-1 contributed to the postprandial stimulation of insulin secretion. Accordingly, lack of endogenous IL-1 signaling in mice during refeeding and obesity diminished the concentration of insulin in plasma. IL-1 and insulin increased the uptake of glucose into macrophages, and insulin reinforced a pro-inflammatory pattern via the insulin receptor, glucose metabolism, production of reactive oxygen species, and secretion of IL-1 mediated by the NLRP3 inflammasome. Postprandial inflammation might be limited by normalization of glycemia, since it was prevented by inhibition of the sodium-glucose cotransporter SGLT2. Our findings identify a physiological role for IL-1 and insulin in the regulation of both metabolism and immunity.

DOI: <https://doi.org/10.1038/ni.3659>

Posted at the Zurich Open Repository and Archive, University of Zurich

ZORA URL: <https://doi.org/10.5167/uzh-133189>

Journal Article

Accepted Version

Originally published at:

Dror, Erez; Dalmas, Elise; Meier, Daniel T; Wueest, Stephan; Thévenet, Julien; Thienel, Constanze; Timper, Katharina; Nordmann, Thierry M; Traub, Shuyang; Schulze, Friederike; Item, Flurin; Vallois, David; Pattou, Francois; Kerr-Conte, Julie; Lavallard, Vanessa; Berney, Thierry; Thorens, Bernard; Konrad, Daniel; Böni-Schnetzler, Marianne; Donath, Marc Y (2017). Postprandial macrophage-derived IL-1 stimulates insulin, and both synergistically promote glucose disposal and inflammation. *Nature Immunology*, 18(3):283-292.

DOI: <https://doi.org/10.1038/ni.3659>

22 **Abstract**

23 The deleterious role of chronic activation of the IL-1 β system in type 2 diabetes and other
24 metabolic diseases is well documented. However, a possible physiological role of IL-1 β in
25 glucose metabolism remained unexplored. Here we show that feeding induces a
26 physiological increase in the number of peritoneal macrophages, which secrete IL-1 β in a
27 glucose-dependent manner. Subsequently, IL-1 β contributes to postprandial stimulation of
28 insulin secretion. Accordingly, lack of endogenous IL-1 β in mice during refeeding and obesity
29 reduced plasma insulin. IL-1 β and insulin increased glucose uptake into macrophages, and
30 insulin reinforced a pro-inflammatory pattern via the insulin receptor, glucose metabolism,
31 reactive oxygen species production, and NLRP3 inflammasome-mediated IL-1 β secretion.
32 Post-prandial inflammation is limited by normalization of glycemia and can be prevented by
33 inhibition of sodium-glucose cotransporter 2 (SGLT2). Our findings identify a physiological
34 role for IL-1 β and insulin in the regulation of both metabolism and immunity.

35

36 Introduction

37 Activation of the innate immune system is an initial response of the body to infections and
38 injuries. The resulting inflammation aims at protecting against stressors and at restoring
39 tissue and organism homeostasis. This process is largely driven by IL-1 β , one of the first
40 described cytokines¹. However, prolonged activation of the immune system by over-
41 nutrition may eventually promote the development of metabolic diseases²⁻⁶. A critical sensor
42 of nutrient overload is the NLRP3 inflammasome, which processes pro-IL-1 β to its active
43 form in various metabolic disorders. This is the case for uric acid crystals which activate the
44 NLRP3 inflammasome in gout⁷, for cholesterol crystals in atherogenesis⁸, and for glucose,
45 fatty acids and islet amyloid polypeptide in type 2 diabetes⁹⁻¹³. Importantly, a causal link
46 between IL-1 β -induced inflammation and these metabolic diseases has been demonstrated
47 by various genetic and pharmacological approaches in animal models¹⁴⁻¹⁶ and in clinical
48 trials¹⁷⁻²¹. While these studies shed light on the pathological role of IL-1 β in metabolism, a
49 physiological function of IL-1 β in metabolic control remains largely unexplored.

50

51 In response to pathogens and obesity, profound changes in the metabolism of immune cells
52 take place²²⁻²⁵. Beyond supplying energy, nutrients can also act as signaling molecules that
53 promote the activation of immune cells. Indeed, elevated glucose and other metabolites
54 drive production of IL-1 β by macrophages^{14,26}.

55

56 Insulin-producing β cells have the highest IL-1 receptor expression of any tissue²⁷ and the IL-
57 1 receptor is the most abundantly expressed cell surface receptor on β cells²⁸, pointing to a
58 hitherto unappreciated physiological function. While the deleterious role of high-dose and
59 long-term IL-1 β exposure on islet function and mass is well documented^{29,30}, a few mainly *in*
60 *vitro* observations hint to a possible beneficial role of IL-1 β in insulin secretion and β -cell
61 survival^{31,32}.

62

63 Parenteral glucose stimulation leads to a rapid first and second phase of insulin release. In
64 contrast, the physiological slower resorption of a meal elicits a sustained increase of insulin
65 that depends on the duration of food intake³³. Thereby the insulin response to enteral food
66 intake cannot be solely accounted for by the associated changes in blood glucose. It is
67 modulated by several insulin secretagogues including the incretin hormones GIP and GLP-
68 1³⁴. These hormones promote insulin secretion only when glucose levels are elevated. While
69 GIP and GLP-1 are the best described incretins, other incretin-like factors are thought to
70 exist.

71

72 Several studies show that food intake transiently induces a mild inflammatory response^{35,36}.
73 We hypothesized that IL-1 β contributes to this postprandial inflammation, regulating whole
74 body glucose homeostasis along with an innate immune response. Thereby, it may deliver
75 the energy needed to activate the innate immune system in order to prevent the
76 dissemination of microorganisms contained in the food. We show here that a postprandial
77 rise in glucose leads to acute elevation of macrophage-derived IL-1 β , which contributes to
78 postprandial insulin secretion via the abundantly expressed IL-1 receptor on β cells. Insulin
79 reinforces a pro-inflammatory state and stimulates macrophages to produce IL-1 β via
80 glucose metabolism, subsequent production of reactive oxygen species (ROS) which leads to
81 activation of the inflammasome^{14,37}. Both, insulin and IL-1 β regulate glucose disposal,
82 whereby IL-1 β preferentially stimulates glucose uptake into the immune cell compartment.

83

84 **Results**

85

86 **Feeding stimulates intra-peritoneal macrophages to produce IL-1 β .**

87 In order to study the physiological involvement of IL-1 β in insulin secretion we performed
88 overnight fasting followed by refeeding experiments in wild-type and *IL1b*^{-/-} mice. Two hours
89 after refeeding, circulating IL-1 β concentration was increased in wild-type mice, while, as
90 expected, IL-1 β remained undetectable in *IL1b*^{-/-} mice (**Fig. 1a**; for validation of the assay see
91 **Supplementary Fig. 1a**). Of note, IL-1 β concentration in serum was already elevated 30
92 minutes after refeeding (not shown). Next we investigated the source of increased IL-1 β .
93 Following refeeding, expression of *Il1b* mRNA and of the IL-1 β -dependent chemokines *Cxcl1*
94 and *Ccl2* were increased in the omental fat (the main site from which macrophages migrate
95 into the peritoneum^{38,39}; **Fig. 1b**) but not in the circulating leukocytes, liver, spleen,
96 epididymal fat or subcutaneous fat (not shown). Furthermore, the number of stromal
97 vascular cells isolated from the omentum was reduced (fasted: $41.8 \pm 13.4 \times 10^3$ cells/mg;
98 refed: $8.3 \pm 2.6 \times 10^3$ cells/mg; mean \pm s.e.m.). Accordingly, we observed a marked increase
99 in the number of peritoneal cells (**Fig. 1c**), which displayed an increase in *Il1b* mRNA
100 expression (**Fig. 1d**). Flow cytometry revealed that the majority of these cells were
101 macrophages (**Fig. 1e**; for gating strategy see **Supplementary Fig. 1b**), a repartition that
102 remained unchanged between fasting and refeeding (not shown). *Ex vivo*, spontaneous
103 release of IL-1 β by cultured peritoneal macrophages from fasted or refed mice was
104 comparable (not shown). However, macrophages from refed mice released more IL-1 β
105 following stimulation with ATP (**Fig. 1f**). To validate the source of the increased IL-1 β during
106 refeeding, we generated *Il1b*^{fl/fl}Lyz2-Cre mice, which specifically lack IL-1 β in the myeloid
107 lineage (**Supplementary fig. 1c**). Two hours after refeeding, circulating IL-1 β concentration
108 was increased in wild-type mice but not in their *Il1b*^{fl/fl}Lyz2-Cre littermates (**Fig 1g**). We then
109 tested whether the increase in serum glucose following feeding mediated the postprandial

110 increase in IL-1 β . We treated mice with the SGLT2 inhibitor canagliflozin, which decreases
111 glycemia via inhibition of renal glucose reabsorption. Treatment of mice with canagliflozin
112 induced glycosuria and prevented postprandial increase in glucose and insulin
113 (**Supplementary Fig. 1d-f**), along with a complete prevention of postprandial increase in
114 circulating IL-1 β (**Fig. 1h**). Similarly, injection of the non-metabolizable glucose analogue 2-
115 deoxyglucose (2DG) prior to refeeding strongly reduced IL-1 β release (**Fig. 1i**). Finally, we
116 tested the role of bacterial products in the stimulation of postprandial IL-1 β by treating mice
117 with broad-spectrum antibiotics or lipopolysaccharide (LPS). Antibiotics-treated mice tended
118 to have milder postprandial inflammation than untreated mice as detected by *Il1b* and *Cxcl1*
119 gene expression in the omental fat pad (**Supplementary Fig. 1g, h**) together with a mild
120 decrease in postprandial circulating IL-1 β (**Supplementary Fig. 1i**) despite similar food intake
121 and no change in the number of peritoneal cells (**Supplementary Fig. 1j-l**). *Ex vivo*,
122 peritoneal macrophages from antibiotic-treated mice released less IL-1 β , even in the
123 presence of ATP (**Fig. 1j**). However, priming with LPS prior to ATP stimulation restored IL-1 β
124 secretion (**Fig. 1j**). Accordingly, *in vivo* i.p. injection of LPS into fed mice increased circulating
125 IL-1 β along with insulin and decreased blood glucose (**Fig. 1k**). However, injection of LPS in
126 genomic *Il1b*^{-/-} mice failed to induce insulin (**Fig. 1l**). This suggests that there is a need for a
127 microbial-related stimulus and energy supply (glucose) to induce postprandial release of IL-
128 1 β . Thus, feeding increases the number of intra-peritoneal macrophages, which are primed
129 by bacterial products to produce and release IL-1 β in response to glucose.

130

131 **Postprandial macrophage IL-1 β promotes insulin secretion.**

132 Next, we examined the direct effect of elevated IL-1 β after refeeding on insulin secretion.
133 First, we measured postprandial circulating insulin in littermate *Il1b*^{-/-} or wild-type refeed
134 mice. *Il1b*^{-/-} mice had reduced insulin secretion (**Fig. 2a**) and elevated blood glucose
135 (**Supplementary Fig. 2a**) after refeeding compared to wild-type mice, despite comparable

136 food intake (not shown). Since the number of peritoneal cells was increased upon refeeding
137 (**Fig. 1c**), and macrophages are the most abundant immune cells in the peritoneal cavity (**Fig.**
138 **1e**), we depleted macrophages in wild-type mice by i.p. injection of clodronate
139 (**Supplementary Fig. 2b**) prior to performing fasting-refeeding experiments. Depletion of
140 macrophages resulted in a marked decreased of postprandial insulin in the circulation (**Fig.**
141 **2b**). Similarly, postprandial insulin was lower in *Il1b^{fl/fl}* *Lyz2-Cre* mice compared to their wild-
142 type littermates (**Fig. 2c**). In addition, acute blockade of IL-1 with its natural antagonist IL-
143 1Ra prior to refeeding resulted in slightly decreased circulating insulin in wild-type mice (**Fig.**
144 **2d**) and elevated blood glucose (**Supplementary Fig. 2c**). Since obesity is associated with
145 inflammation and chronically elevated IL-1 β and insulin⁹, we investigated the effect of acute
146 (1 hour before refeeding) IL-1 antagonism in diet- induced obese (DIO) mice to substantiate
147 the ability of endogenous IL-1 β to regulate insulin. Blocking the elevated circulating levels of
148 IL-1 β (**Fig. 2e**) with IL-1Ra lowered fasting insulin levels in DIO mice (**Fig. 2f**) without
149 changing insulin sensitivity or hepatic glucose production as determined by a
150 hyperinsulinemic-euglycemic clamp (**Fig. 2g, h**). As a second model, genetically obese db/db
151 mice were injected with IL-1Ra, which also decreased insulin levels (**Fig. 2i**). Therefore,
152 postprandial IL-1 β derived from myeloid cells promotes insulin secretion.

153

154 **Acute exposure to IL-1 β induces insulin secretion.**

155 To directly test the effect of IL-1 β on insulin secretion *in vivo*, we performed acute injections
156 of IL-1 β in mice followed by i.p. glucose tolerance test (GTT). IL-1 β led to a marked elevation
157 in insulin secretion (**Fig. 3a**) and improved glucose tolerance (**Fig. 3b**). Insulin was also
158 increased and glycemia improved by IL-1 β administration in the absence of a glucose bolus
159 but to a much lesser extent (**Fig. 3c, d**; note the different scale in the y-axis compared to **3a**
160 **& b**). This glucose-dependent potentiation of insulin secretion is reminiscent of effects
161 elicited by the incretin hormones GLP-1 and GIP³⁴. However, circulating active GLP-1

162 concentrations remained unchanged following IL-1 β injections (**Supplementary Fig. 3a**).
163 Furthermore, the effect of IL-1 β on insulin secretion and glucose tolerance was identical in
164 *Glp1r*^{-/-}/*Gipr*^{-/-} double knock-out mice compared to their wild-type littermates
165 (**Supplementary Fig. 3b, c**) and treatment of mice with the GLP-1 inhibitor Exendin fragment
166 9-39 did not reduce the IL-1 β effect on insulin secretion (not shown). Therefore, IL-1 β did
167 not promote glucose-induced insulin secretion via incretin hormones. Since insulin secretion
168 could be increased as a result of IL-1 β -mediated peripheral insulin resistance, we
169 determined if insulin sensitivity changes upon an acute IL-1 β injection using insulin tolerance
170 tests and hyperinsulinemic-euglycemic clamp studies. Acute injection of IL-1 β had no effect
171 on insulin sensitivity or hepatic glucose production (**Fig. 3e, Supplementary Fig. 3d**). IL-1 β
172 also improved glucose tolerance and strongly increased insulin secretion in DIO mice (**Fig. 3f,**
173 **g**) and in genetically obese db/db mice (**Fig. 3h, i**). In contrast to wild-type mice, *interleukin 1*
174 *receptor-associated kinase 4* (*Irak4*^{-/-}) deficient mice injected with IL-1 β before an i.p. GTT
175 showed no improvement in insulin secretion and no change in glycemia (**Supplementary Fig.**
176 **3e, f**) demonstrating that the observed effects of IL-1 β are mediated by the IL-1 receptor
177 signal transduction pathways. Of note, i.p. injection of 0.1 μ g/kg of IL-1 β resulted in
178 circulating IL-1 β concentrations similar to those obtained upon refeeding and also induced
179 insulin secretion (**Fig. 3j, k**). Next we tested whether LPS has similar effects. Acute i.p. LPS
180 injection improved glucose tolerance and increased insulin secretion in both wild-type and
181 DIO mice (**Fig. 4a, b**). Importantly, IL-1Ra treatment blocked LPS-induced insulin secretion
182 (**Fig. 4c**). Type 1 IL-1 receptor mRNA (*Il1r1*) was expressed at a much higher level in isolated
183 endocrine cells than in islet resident immune or endothelial cells (**Fig. 4d**). Specific
184 immunostaining of mouse pancreatic tissue sections revealed the presence of IL-1R1 in a
185 subpopulation of β cells (**Fig. 4e**). Previous *in vitro* studies³² demonstrated that very low
186 concentrations of IL-1 β increased glucose-stimulated insulin secretion from islets. We
187 confirmed this effect in mouse and human islets, and with the human β -cell line ENDOC

188 (Supplementary Fig. 3g-i), suggesting a direct β -cell effect. To determine whether acute
189 administration of IL-1 β , *in vivo*, acts directly on the islet, we used streptozotocin (STZ) to
190 eliminate β cells from recipient mice and transplanted them with islets from wild-type or
191 *Il1r1*^{-/-} donor mice. The effect of IL-1 β on insulin secretion and glucose tolerance was lost in
192 *Il1r1*^{-/-} transplanted mice (Fig. 4f, g). These results suggest that systemic IL-1 β potentiates
193 glucose-induced insulin secretion via islet IL-1R1, and this is independent of the incretins
194 GLP-1 and GIP or of changes in insulin resistance.

195

196 **Insulin stimulates IL-1 β secretion of macrophages**

197 Since IL-1 β enhanced insulin secretion during refeeding, we investigated the possible
198 synergistic contribution of insulin and IL-1 β to the stimulation of the immune system. First
199 we investigated by flow cytometry the expression of the insulin receptor (InsR) on resident
200 macrophages isolated from several tissues. We found that peritoneal macrophages had the
201 highest insulin receptor expression compared to other resident macrophages (Fig 5a).
202 Moreover, we found that the InsR was upregulated in peritoneal macrophages from DIO
203 mice (Fig. 5b) and in the pro-inflammatory M1 compared to naive M0 macrophages,
204 whereas it was mildly downregulated in anti-inflammatory M2 macrophages (Fig. 5c,
205 Supplementary Fig. 4a). Accordingly, insulin induced AKT phosphorylation in naive M0, to a
206 greater extent in M1 and not in M2 macrophages (Fig. 5d, Supplementary Fig.4b). The
207 insulin effect on AKT phosphorylation was confirmed using a quantitative multiplex assay
208 (Fig. 5e). In contrast to the PI3K activation pathway, insulin had no impact on MAPK
209 signaling (Fig. 5f). Insulin also stimulated upregulation of the glucose transporter *Slc2a1*
210 (encodes GLUT1, the isoform that is mainly expressed in immune cells²⁵; Fig. 5g) and the
211 expression of hexokinase 2 (*Hk2*), the rate-limiting enzyme in glycolysis (Fig. 5h), in M1
212 macrophages. In line with this pattern, a 2 hour insulin treatment increased glycolytic
213 activity in M1 macrophages, but not in naive or M2 macrophages (Fig. 5i, Supplementary

214 **Fig. 4c).** In accordance with the phosphorylation assay, the AKT signaling inhibitor LY294002
215 but not the MAPK signaling inhibitor U0126 blocked the effect of insulin on glycolytic activity
216 in M1 macrophages (**Fig. 5j**). Further, insulin induced glucose uptake in naive macrophages,
217 and this effect was enhanced by IL-1 β (**Fig 5k**). Similar to the pattern of insulin receptor
218 expression and activation, insulin induced secretion of mature IL-1 β preferentially in M1
219 macrophages in an NLRP3-dependent manner (**Fig. 6a**). Insulin also stimulated *Tnf*, *Il6*, and
220 *Cxcl1* expression and protein release in M1 macrophages but independently of NLRP3
221 activation (**Supplementary Fig. 4d, e**). This insulin effect on IL-1 β appeared to be
222 independent of cell death and survival, which remained unaffected (**Supplementary Fig. 4f**).
223 Similar to insulin-induced glycolysis, insulin stimulated IL-1 β via the PI(3)K activation
224 pathway and was blocked by LY294002 and downstream by the mTOR inhibitor rapamycin
225 (**Fig. 6b**). We then tested the role of glucose metabolism in insulin-induced IL-1 β secretion.
226 First, the GLUT1 inhibitor fasentin blocked IL-1 β secretion (**Fig. 6c**). In addition, insulin failed
227 to induce IL-1 β when cells were cultured with the non-metabolizable glucose analogue 2DG
228 or with the mitochondria targeted ROS scavenger Mito-TEMPO (**Fig. 6d**). IL-1Ra was
229 undetectable following short-term exposure (2 hours) to insulin (not shown) however
230 prolonged (12 hours) exposure to insulin induced IL-1Ra in M0 and M1 macrophages
231 indicating that the induction of IL-1 β was later counterbalanced by IL-1Ra secretion (**Fig. 6e,**
232 **f**). Similarly to our *in vitro* data, acute injection of insulin in mice increased amounts of
233 circulating IL-1 β and CXCL1 (**Fig. 6g, Supplementary Fig. 4g**). Overall, these data show that
234 insulin induces inflammasome-mediated IL-1 β secretion via enhanced glucose metabolism
235 and mitochondrial ROS production. These effects are dependent on the AKT/-PI(3)K pathway
236 and on the activity status of the macrophages.

237

238 **IL-1 β shifts glucose uptake to immune cells**

239 Next, we tested how IL-1 β contributes to glucose disposal. Exposure of macrophages to IL-
240 1 β led to an increase in glucose uptake (**Fig. 7a**), while blocking endogenously produced IL-1
241 with IL-1Ra slightly decreased glucose uptake (**Fig. 7b**). We then examined the effect of IL-1 β
242 and insulin injection on glucose uptake in wild-type mice. To avoid glucose-stimulated
243 insulin secretion, we only used trace amounts of non-metabolizable radiolabeled glucose. IL-
244 1 β stimulated glucose uptake in spleen and circulating leukocytes (**Fig. 7c, d**). IL-1 β also
245 increased glucose uptake in adipose tissue and in muscle, however to a lesser extent than
246 insulin (**Fig. 7e-g**). This is potentially due to the mild stimulation of insulin secretion by IL-1 β
247 observed in the absence of a glucose bolus (**Fig. 3c**). To mimic the chronic elevation of IL-1 β ,
248 we injected mice with IL-1 β daily for 3 consecutive days and determined the number and
249 glucose uptake of peritoneal cells. Similar to refed mice, IL-1 β -injected mice had more
250 peritoneal cells (**Fig. 7h**). *Ex vivo*, glucose uptake of macrophages from these mice was
251 increased (**Fig. 7i**). To test the physiological relevance of IL-1 β -induced glucose uptake, we
252 investigated postprandial glucose uptake in immune cells of refed mice. Blockade of
253 endogenous IL-1 with IL-1Ra decreased glucose uptake in peritoneal macrophages (**Fig. 7j**).
254 To further examine the contribution of immune cells to overall body glucose disposal, we
255 first used T and B cell deficient (*Rag2*^{-/-}) mice. A single injection of IL-1 β prior to a GTT in
256 *Rag2*^{-/-} mice lowered glucose concentration as potently as in littermate control mice
257 (**Supplementary Fig. 5a**). Since *Rag2*^{-/-} mice have a compensatory increase in the number of
258 macrophages, we additionally ablated macrophages in *Rag2*^{-/-} mice with clodronate
259 liposomes (**Supplementary Fig. 5b**). This diminished the profound beneficial effect of IL-1 β
260 on glucose disposal, despite increased insulin levels (**Fig. 7k**), suggesting that immune cells
261 substantially contribute to IL-1 β -induced glucose disposal. Thus, beside the stimulation of
262 insulin, IL-1 β directly regulates glycemia by promotion of glucose disposal preferentially in
263 immune cells (**Supplementary Fig. 6**).

264

265 Discussion

266 In the present study we show that feeding induces a physiological elevation of macrophage-
267 derived IL-1 β that promotes postprandial insulin secretion. This effect depends on bacterial
268 products, which primes macrophages to produce more pro-IL-1 β , and on glucose that drives
269 the maturation of IL-1 β . The production of IL-1 β by M1, and to a lesser extent by M0,
270 macrophages is enhanced by insulin. Insulin upregulates functional insulin receptors,
271 signaling via the AKT/-PI(3)K pathway, glucose uptake through the glucose transporter
272 GLUT1, glucose metabolism, and ROS production that activates the NLRP3
273 inflammasome^{14,37}. Both insulin and IL-1 β regulate whole body glucose disposal by
274 promoting glucose uptake in muscle and fat, and fuel the immune system by stimulating
275 glucose uptake into the immune cell compartment. Ablation of macrophages in T- and B-cell
276 deficient mice significantly reduced IL-1 β -mediated glucose clearance. Self-amplification of
277 the system is limited by normalization of glycemia.

278

279 The number of macrophages in the peritoneum was increased upon refeeding along with
280 increased expression of inflammatory genes including *Il1b* in omental fat, which supports
281 active trafficking of macrophages into the peritoneal cavity⁴⁰. Therefore, feeding stimulates
282 immune surveillance, possibly to limit the dissemination of microorganisms contained in
283 food. Activation of the immune system requires energy and contributes substantially to
284 whole-body glucose consumption. We provide evidence that both, bacterial products and
285 glucose metabolism, are required to induce postprandial IL-1 β secretion by peritoneal
286 macrophages. Indeed, we show that peritoneal cells from refed mice have elevated *Il1b*
287 mRNA levels. This might rather be promoted by translocation of ingested or intestinal
288 bacterial products than by the microbiota itself⁴¹⁻⁴³, since pretreatment of mice with
289 antibiotics before refeeding only mildly lowered IL-1 β secretion. However, stimulation of IL-
290 1 β release strongly depends on glucose uptake and metabolism. Indeed, we observed that

291 decreasing glycemia via SGLT2 inhibition or blocking glycolysis with 2DG prevented
292 postprandial IL-1 β in the circulation. This suggests that from all factors that could mediate
293 this effect during feeding, such as mechanical stress of the digestive system, fiber, amino
294 acid and fat intake, it is mainly glucose that drives IL-1 β secretion. Our results also suggest a
295 role for insulin in postprandial IL-1 β secretion since insulin increased glucose uptake and
296 metabolism in macrophages. Inhibition of glucose uptake with fasentin or 2DG blocked
297 insulin-induced IL-1 β secretion. Downstream, inhibiting mitochondrial ROS production,
298 which activates the NLRP3 inflammasome^{14,37}, also prevented insulin from inducing IL-1 β .

299

300 Previous *in vitro* studies have shown that low concentrations of IL-1 β mildly stimulate insulin
301 secretion³². Here we show that *in vivo*, IL-1 β injections strongly potentiate insulin secretion
302 in the presence of a glucose bolus. However, the most natural way to stimulate insulin
303 secretion is eating. We find that IL-1 β -induced insulin release occurs in physiology by
304 demonstrating that postprandially produced IL-1 β increased insulin levels and decreased
305 glycemia. This IL-1 β effect is partly mediated by the highly expressed IL-1R1 on β -cells, since
306 the effect of IL-1 β on insulin secretion and glucose tolerance was blunted in diabetic mice
307 transplanted with islets from *Il1r1*^{-/-} mice.

308

309 The beneficial effects of postprandial IL-1 β on glucose homeostasis are in apparent contrast
310 to the glucose lowering effects of IL-1 antagonism in patients with type 2 diabetes¹⁷ and to
311 the well-described deleterious effects of IL-1 β on islet function and survival⁴. Though IL-1 β
312 provokes β -cell demise^{30,44}, at low concentrations or upon short exposure, IL-1 β
313 paradoxically stimulates β -cell proliferation and decreases apoptosis³². Therefore, IL-1 β is
314 not only detrimental for β -cells but has more complex biological functions⁴⁵. An explanation
315 to reconcile the beneficial effects of IL-1 blockade in type 2 diabetes is the difference
316 between acute and chronic effects and the concept of β -cell “rest”. Indeed, potassium

317 channel openers, which decrease insulin secretion, ultimately improve insulin secretion in
318 patients with type 2 diabetes⁴⁶. The benefit of IL-1 antagonism in patients with type 2
319 diabetes could result from β -cell rest, possibly in combination with inhibition of the toxic
320 effects of IL-1 β .

321

322 A further explanation why chronic upregulation of IL-1 β leading to elevated insulin levels
323 may become unfavorable for metabolism stems from our observation that insulin reinforces
324 the inflammatory state of macrophages through enhanced glucose uptake and metabolism
325 and increased InsR expression in macrophages of DIO mice. Indeed, activated macrophages
326 play a crucial role in insulin resistance⁴⁷. In line with this, insulin receptor expression was
327 also higher in macrophages from DIO mice, where macrophages have been shown to be pro-
328 inflammatory⁶. Thus, we propose that insulin, which is increased in early stages of type 2
329 diabetes, may drive and sustain the inflammatory state in macrophages and may therefore
330 contribute to the chronic low-grade inflammation associated with metabolic diseases.
331 Thereby, TNF α , IL-6 and CXCL1 may also add to the effect of IL-1 β . In support, myeloid cell-
332 restricted InsR deficient mice are protected against metabolic inflammation and insulin
333 resistance⁴⁸.

334

335 The effect of insulin in macrophages was previously studied without taking into account the
336 polarization status of the macrophages⁴⁹. Herein we show that insulin preferentially acts on
337 pro-inflammatory M1 macrophages characterised by more InsRs, enhanced downstream
338 AKT phosphorylation and glycolytic activity. Further insulin promotes the NLRP3
339 inflammasome and leads to macrophage-derived IL-1 β release. Interestingly, peritoneal
340 macrophages had the highest insulin receptor density, supporting their contribution to
341 postprandial homeostasis.

342

343 SGLT2 inhibitors have recently been approved for the treatment of type 2 diabetes and the
344 EMPA-REG outcome study revealed an impressive reduction in mortality⁵⁰. However the
345 mechanisms leading to this protective effect are unclear. In the present study, we show that
346 canagliflozin prevents postprandial IL-1 β elevation in the circulation. This could be due to
347 increased glucose excretion in the urine, which prevents an overload of glucose in tissues,
348 thereby avoiding deleterious chronic effects of glucose-induced IL-1 β .

349

350 Altogether, our findings show that IL-1 β , a master regulator of inflammation, and insulin, a
351 key hormone in glucose metabolism, promote each other. Both have potent effects on
352 glucose homeostasis and on the activity of the immune system, supporting the emerging
353 concept that inflammatory mediators play a role not only in the pathology of metabolism
354 but are an integral part of its physiology. The physiological synergy between IL-1 β and
355 insulin on glucose disposal may be required to cope with the concomitant challenge by
356 nutrients and microorganisms related to food intake.

357

358 **Accession Codes**

359 Not applicable

360

361 **Data Availability Statement**

362 The data that support the findings of this study are available from the corresponding author

363 upon request.

364 **Acknowledgments**

365 This work was financially supported by the Swiss National Research Foundation (166519 to
366 M.Y.D.) and the European Genomic Institute for Diabetes (ANR-10-LABX-46 to F.P.). We
367 thank our technicians M. Borsigova, K. Dembinski and S. Haeuselmann for excellent technical
368 assistance, S. Dimeloe, E. Traunecker, and D. Labes for technical advice, G. Bantug for
369 technical and editorial advice, the center for transgenic models of the University of Basel
370 and D. Klewe-Nebenius for supporting the production of the *Il1b^{fl/fl}* mouse.

371

372 **Author Contributions**

373 E.Dr., M.B.S and M.Y.D designed the study and wrote the manuscript; E.Dr. performed and
374 analyzed most of the experiments. M.B.S, E.Da, and D.T.M performed and analyzed
375 experiments; C.T, K.T, T.N, S.T, F.S, and D.V helped with experiments. S.W, F.I, and D.K
376 performed the clamps. J.T, F.P, J.K.C provided human islets and performed the islet
377 transplantation experiments. V.L. and T.B provided human islets. B.T provided the *Gipr^{-/-}*
378 */Glp1r^{-/-}* mice; all co-authors helped with the manuscript. M.Y.D and M.B.S supervised the
379 Research.

380

381 **Competing Financial Interests Statement**

382 M.Y.D. is listed as the inventor on a patent filed in 2003 for the use of an interleukin-1
383 receptor antagonist for the treatment of, or prophylaxis against, type 2 diabetes

384

385 **References**

- 386 1. Dinarello, C.A. Multiple biological properties of recombinant human interleukin 1
387 (beta). *Immunobiology* **172**, 301-315 (1986).
- 388 2. Wellen, K.E. & Hotamisligil, G.S. Inflammation, stress, and diabetes. *The Journal of*
389 *clinical investigation* **115**, 1111-1119 (2005).
- 390 3. Hotamisligil, G.S., Shargill, N.S. & Spiegelman, B.M. Adipose expression of tumor
391 necrosis factor-alpha: direct role in obesity-linked insulin resistance. *Science* **259**, 87-
392 91 (1993).
- 393 4. Donath, M.Y., Dalmas, E., Sauter, N.S. & Boni-Schnetzler, M. Inflammation in obesity
394 and diabetes: islet dysfunction and therapeutic opportunity. *Cell metabolism* **17**,
395 860-872 (2013).
- 396 5. Ehses, J.A., Boni-Schnetzler, M., Faulenbach, M. & Donath, M.Y. Macrophages,
397 cytokines and beta-cell death in Type 2 diabetes. *Biochemical Society transactions*
398 **36**, 340-342 (2008).
- 399 6. Donath, M.Y. & Shoelson, S.E. Type 2 diabetes as an inflammatory disease. *Nature*
400 *reviews. Immunology* **11**, 98-107 (2011).
- 401 7. Martinon, F., Petrilli, V., Mayor, A., Tardivel, A. & Tschopp, J. Gout-associated uric
402 acid crystals activate the NALP3 inflammasome. *Nature* **440**, 237-241 (2006).
- 403 8. Duewell, P., *et al.* NLRP3 inflammasomes are required for atherogenesis and
404 activated by cholesterol crystals. *Nature* **464**, 1357-1361 (2010).
- 405 9. Vandanmagsar, B., *et al.* The NLRP3 inflammasome instigates obesity-induced
406 inflammation and insulin resistance. *Nature medicine* **17**, 179-188 (2011).
- 407 10. Wen, H., *et al.* Fatty acid-induced NLRP3-ASC inflammasome activation interferes
408 with insulin signaling. *Nature immunology* **12**, 408-415 (2011).
- 409 11. Stienstra, R., *et al.* The inflammasome-mediated caspase-1 activation controls
410 adipocyte differentiation and insulin sensitivity. *Cell metabolism* **12**, 593-605 (2010).

- 411 12. Maedler, K., *et al.* Glucose-induced beta cell production of IL-1beta contributes to
412 glucotoxicity in human pancreatic islets. *The Journal of clinical investigation* **110**,
413 851-860 (2002).
- 414 13. Masters, S.L., *et al.* Activation of the NLRP3 inflammasome by islet amyloid
415 polypeptide provides a mechanism for enhanced IL-1beta in type 2 diabetes. *Nature*
416 *immunology* **11**, 897-904 (2010).
- 417 14. Zhou, R., Tardivel, A., Thorens, B., Choi, I. & Tschopp, J. Thioredoxin-interacting
418 protein links oxidative stress to inflammasome activation. *Nature immunology* **11**,
419 136-140 (2010).
- 420 15. Stienstra, R., *et al.* Inflammasome is a central player in the induction of obesity and
421 insulin resistance. *Proceedings of the National Academy of Sciences of the United*
422 *States of America* **108**, 15324-15329 (2011).
- 423 16. Ehses, J.A., *et al.* IL-1 antagonism reduces hyperglycemia and tissue inflammation in
424 the type 2 diabetic GK rat. *Proceedings of the National Academy of Sciences of the*
425 *United States of America* **106**, 13998-14003 (2009).
- 426 17. Larsen, C.M., *et al.* Interleukin-1-receptor antagonist in type 2 diabetes mellitus. *The*
427 *New England journal of medicine* **356**, 1517-1526 (2007).
- 428 18. van Asseldonk, E.J., *et al.* Treatment with Anakinra improves disposition index but
429 not insulin sensitivity in nondiabetic subjects with the metabolic syndrome: a
430 randomized, double-blind, placebo-controlled study. *The Journal of clinical*
431 *endocrinology and metabolism* **96**, 2119-2126 (2011).
- 432 19. Cavelti-Weder, C., *et al.* Effects of gevokizumab on glycemia and inflammatory
433 markers in type 2 diabetes. *Diabetes care* **35**, 1654-1662 (2012).
- 434 20. Hensen, J., Howard, C.P., Walter, V. & Thuren, T. Impact of interleukin-1beta
435 antibody (canakinumab) on glycaemic indicators in patients with type 2 diabetes

436 mellitus: results of secondary endpoints from a randomized, placebo-controlled
437 trial. *Diabetes & metabolism* **39**, 524-531 (2013).

438 21. Sloan-Lancaster, J., *et al.* Double-blind, randomized study evaluating the glycemic
439 and anti-inflammatory effects of subcutaneous LY2189102, a neutralizing IL-1beta
440 antibody, in patients with type 2 diabetes. *Diabetes care* **36**, 2239-2246 (2013).

441 22. Gubser, P.M., *et al.* Rapid effector function of memory CD8+ T cells requires an
442 immediate-early glycolytic switch. *Nature immunology* **14**, 1064-1072 (2013).

443 23. Fox, C.J., Hammerman, P.S. & Thompson, C.B. Fuel feeds function: energy
444 metabolism and the T-cell response. *Nature reviews. Immunology* **5**, 844-852 (2005).

445 24. Macintyre, A.N., *et al.* The glucose transporter Glut1 is selectively essential for CD4 T
446 cell activation and effector function. *Cell metabolism* **20**, 61-72 (2014).

447 25. Freerman, A.J., *et al.* Metabolic reprogramming of macrophages: glucose
448 transporter 1 (GLUT1)-mediated glucose metabolism drives a proinflammatory
449 phenotype. *The Journal of biological chemistry* **289**, 7884-7896 (2014).

450 26. Tannahill, G.M., *et al.* Succinate is an inflammatory signal that induces IL-1beta
451 through HIF-1alpha. *Nature* **496**, 238-242 (2013).

452 27. Boni-Schnetzler, M., *et al.* Free fatty acids induce a proinflammatory response in
453 islets via the abundantly expressed interleukin-1 receptor I. *Endocrinology* **150**,
454 5218-5229 (2009).

455 28. Benner, C., *et al.* The transcriptional landscape of mouse beta cells compared to
456 human beta cells reveals notable species differences in long non-coding RNA and
457 protein-coding gene expression. *BMC genomics* **15**, 620 (2014).

458 29. Bendtzen, K., *et al.* Cytotoxicity of human pl 7 interleukin-1 for pancreatic islets of
459 Langerhans. *Science* **232**, 1545-1547 (1986).

460 30. Mandrup-Poulsen, T., *et al.* Affinity-purified human interleukin I is cytotoxic to
461 isolated islets of Langerhans. *Diabetologia* **29**, 63-67 (1986).

- 462 31. Zawalich, W.S. & Zawalich, K.C. Interleukin 1 is a potent stimulator of islet insulin
463 secretion and phosphoinositide hydrolysis. *The American journal of physiology* **256**,
464 E19-24 (1989).
- 465 32. Donath, M.Y., Boni-Schnetzler, M., Ellingsgaard, H., Halban, P.A. & Ehses, J.A.
466 Cytokine production by islets in health and diabetes: cellular origin, regulation and
467 function. *Trends in endocrinology and metabolism: TEM* **21**, 261-267 (2010).
- 468 33. Caumo, A. & Luzi, L. First-phase insulin secretion: does it exist in real life?
469 Considerations on shape and function. *American journal of physiology.*
470 *Endocrinology and metabolism* **287**, E371-385 (2004).
- 471 34. Baggio, L.L. & Drucker, D.J. Biology of incretins: GLP-1 and GIP. *Gastroenterology*
472 **132**, 2131-2157 (2007).
- 473 35. Van Oostrom, A.J., Sijmonsma, T.P., Rabelink, T.J., Van Asbeck, B.S. & Cabezas, M.C.
474 Postprandial leukocyte increase in healthy subjects. *Metabolism: clinical and*
475 *experimental* **52**, 199-202 (2003).
- 476 36. Herieka, M. & Erridge, C. High-fat meal induced postprandial inflammation.
477 *Molecular nutrition & food research* **58**, 136-146 (2014).
- 478 37. Petrilli, V., *et al.* Activation of the NALP3 inflammasome is triggered by low
479 intracellular potassium concentration. *Cell death and differentiation* **14**, 1583-1589
480 (2007).
- 481 38. Okabe, Y. & Medzhitov, R. Tissue-specific signals control reversible program of
482 localization and functional polarization of macrophages. *Cell* **157**, 832-844 (2014).
- 483 39. Platell, C., Cooper, D., Papadimitriou, J.M. & Hall, J.C. The omentum. *World journal*
484 *of gastroenterology : WJG* **6**, 169-176 (2000).
- 485 40. Shrivastava, P. & Bhatia, M. Essential role of monocytes and macrophages in the
486 progression of acute pancreatitis. *World journal of gastroenterology : WJG* **16**, 3995-
487 4002 (2010).

488 41. Cani, P.D., *et al.* Metabolic endotoxemia initiates obesity and insulin resistance.
489 *Diabetes* **56**, 1761-1772 (2007).

490 42. Breton, J., *et al.* Gut Commensal E. coli Proteins Activate Host Satiety Pathways
491 following Nutrient-Induced Bacterial Growth. *Cell metabolism* **23**, 324-334 (2016).

492 43. Zhang, D., *et al.* Neutrophil ageing is regulated by the microbiome. *Nature* **525**, 528-
493 532 (2015).

494 44. Corbett, J.A., Wang, J.L., Sweetland, M.A., Lancaster, J.R., Jr. & McDaniel, M.L.
495 Interleukin 1 beta induces the formation of nitric oxide by beta-cells purified from
496 rodent islets of Langerhans. Evidence for the beta-cell as a source and site of action
497 of nitric oxide. *The Journal of clinical investigation* **90**, 2384-2391 (1992).

498 45. Hajmrle, C., *et al.* Interleukin-1 signaling contributes to acute islet compensation. *JCI*
499 *insight* **1**, e86055 (2016).

500 46. Greenwood, R.H., Mahler, R.F. & Hales, C.N. Improvement in insulin secretion in
501 diabetes after diazoxide. *Lancet* **1**, 444-447 (1976).

502 47. Olefsky, J.M. & Glass, C.K. Macrophages, inflammation, and insulin resistance.
503 *Annual review of physiology* **72**, 219-246 (2010).

504 48. Mauer, J., *et al.* Myeloid cell-restricted insulin receptor deficiency protects against
505 obesity-induced inflammation and systemic insulin resistance. *PLoS genetics* **6**,
506 e1000938 (2010).

507 49. Costa Rosa, L.F., Safi, D.A., Cury, Y. & Curi, R. The effect of insulin on macrophage
508 metabolism and function. *Cell biochemistry and function* **14**, 33-42 (1996).

509 50. Zinman, B., *et al.* Empagliflozin, Cardiovascular Outcomes, and Mortality in Type 2
510 Diabetes. *The New England journal of medicine* **373**, 2117-2128 (2015).

511

512 **Figure legends**

513

514 **Figure 1**

515 **Feeding stimulates intra-peritoneal macrophages to produce IL-1 β .**

516 (a) Circulating IL-1 β in wild-type (WT; n=22, 4 experiments) or *Il1b*^{-/-} (n=3) mice before and
517 after feeding (LLOD denotes the lowest level of detection). (b) Gene expression in omental
518 fat isolated from fasted and refed mice (n=8, 3 experiments). (c) Number of peritoneal cells
519 isolated per mouse (WT, fasted n=15 and refed n=17, 4 experiments). (d) *Il1b* gene
520 expression in peritoneal cells isolated from fasted and refed mice (n=6). (e) Peritoneal cell
521 composition following feeding determined by flow cytometry (pool of 4 refed mice). (f) IL-1 β
522 release of macrophages isolated from fasted (n=5) or refed (n=6) mice and stimulated with
523 ATP. (g-i) Circulating IL-1 β levels before (fasted) or after refeeding (refed) in *Il1b*^{fl/fl}Lyz2-Cre
524 and WT mice (g; n=16 and 15, respectively), in mice treated with or without the SGLT2
525 inhibitor canagliflozin (h; n=13 per group), and in mice treated with or without 2DG (i; saline
526 n=9, 2DG n=10). (j) *Ex vivo* IL-1 β secretion in unstimulated (basal) macrophages isolated
527 from refed mice pretreated for a week with or without antibiotics (ABX, left) or stimulated
528 with ATP (middle) alone or following LPS priming (right). (k) Circulating IL-1 β , insulin, and
529 blood glucose levels after intra-peritoneal (i.p.) injection of LPS (1 mg/kg) in fed mice (n=8).
530 (l) Circulating insulin levels in fed WT or *Il1b*^{-/-} mice after i.p. injection of 1 mg/kg LPS or
531 saline (WT; saline n=5, LPS n=7, *Il1b*^{-/-}; n=7). **P* < 0.05, ***P* < 0.01, ****P* < 0.001, *****P* <
532 0.0001. Statistical significance (*P*) was determined by Student's t test and in (b, g, h, l) by
533 ANOVA. All error bars denote s.e.m.

534

535 **Figure 2**

536 **Postprandial macrophage-derived IL-1 β promotes insulin secretion.**

537 (a) Circulating insulin concentration before (fasted) or after refeeding (refed) in *Il1b*^{-/-} or WT
538 mice (n=6 and 11, respectively). (b, c) Circulating insulin before (fasted) or after refeeding
539 (refed) in (b) WT mice injected with liposomes containing clodronate or PBS (n=17 per
540 group; 3 experiments), and in (c) *Il1b*^{fl/fl} Lyz2-Cre (n=16) and WT (n=15) mice. (d) Circulating
541 insulin following an acute injection of saline or 10 mg/kg IL-1Ra in refed WT mice (n=26 and
542 23, respectively). (e) Basal circulating IL-1 β levels in control (n=8) or DIO (n=10) mice. (f)
543 Circulating insulin following acute injections of saline or 10 mg/kg IL-1Ra in DIO mice (n=15
544 and 13 respectively). Hyperinsulinemic-euglycemic clamp in DIO mice pre-injected with
545 saline or with 10 mg/kg IL-1Ra (n=4 and 5, respectively): (g) Glucose infusion rate, (h) hepatic
546 glucose production. (i) Circulating insulin levels following acute injections of saline or 10
547 mg/kg IL-1Ra in db/db mice (n=4 and 5, respectively). **P* < 0.05, ***P* < 0.01. Statistical
548 significance (*P*) was determined by Student's t test and in (a-c) by ANOVA. All error bars
549 denote s.e.m.

550

551 **Figure 3**

552 **Acute exposure to IL-1 β induces insulin secretion without changing insulin sensitivity.**

553 (a, b) Concentrations of circulating insulin (a) and glucose (b) during an intra-peritoneal
554 glucose tolerance test (i.p. GTT) in WT mice 18 minutes after a single injection with saline or
555 1 μ g/kg IL-1 β (n=5 and 6, respectively). (c, d) Concentrations of circulating insulin (c) and
556 glucose (d) in 6 hour fasted WT mice injected with or without 1 μ g/kg IL-1 β (n=8 per group).
557 (e) Glucose infusion rate and hepatic glucose production during a hyperinsulinemic-
558 euglycemic clamp in WT mice pre-treated with 1 μ g/kg IL-1 β or saline (n=4 and 3,
559 respectively). (f-i) Concentrations of insulin (f, h) and glucose (g, i) during an i.p. GTT in diet-
560 induced obese (DIO) (f, g) and db/db (h, i) mice, pre-treated with 1 μ g/kg IL-1 β (n=12 per
561 group). (j) Circulating IL-1 β concentration and (k) insulin (fold of basal) 18 min after an i.p.
562 injection of 0.1 or 1 μ g/kg of IL-1 β into WT mice (n=9). **P* < 0.05, ***P* < 0.01, ****P* < 0.001,

563 **** $P < 0.0001$. Statistical significance (P) was determined by Student's t test and in (k) by
564 ANOVA. All error bars denote s.e.m.

565

566 **Figure 4**

567 **Systemic IL-1 β potentiates glucose-induced insulin secretion via islet IL-1R1**

568 (a) Circulating insulin and (b) glucose levels during an i.p. GTT in WT and DIO mice 3 hours
569 after a single injection of LPS (1 mg/kg) or saline (n=5 per group). (c) Circulating insulin
570 during an i.p. GTT in WT mice 3 hours after a single injection of saline or LPS (1 mg/kg) with
571 or without IL-1Ra (10 mg/kg; n=5 per group). (d) *Il1r1* mRNA expression in FACS sorted islet
572 cells (n=6 experiments). (e) Double immunostaining of IL-1R1 and insulin in pancreatic tissue
573 sections of WT and *Il1r1*^{-/-} mice. Scale bar, 50 μ m. (f) Circulating insulin and (g) glucose
574 during an i.p. GTT in STZ-treated mice transplanted with WT islets or *Il1r1*^{-/-} islets 18 minutes
575 after a single injection with 1 μ g/kg IL-1 β (n=5 and 4). * $P < 0.05$, ** $P < 0.01$, *** $P < 0.001$,
576 **** $P < 0.0001$. Statistical significance (P) was determined by Student's t test and in (a-d) by
577 ANOVA. All error bars denote s.e.m.

578

579 **Figure 5**

580 **Insulin receptor expression and activation in peritoneal macrophages**

581 (a) Relative mean fluorescence intensity (MFI) of insulin receptor (InsR) protein in different
582 tissue resident macrophages (4 experiments, number of circles indicates number of mice per
583 tissue). (b) Relative MFI of InsR protein in peritoneal macrophages from WT and DIO mice
584 (n=3 mice). (c) *Insr* mRNA expression in naive (M0), pro-inflammatory M1 and alternative
585 M2 polarized macrophages (n=12; 3 experiments). (d) A representative immunoblot of
586 insulin-induced (s473) phospho-AKT in M0, M1 and M2 polarized macrophages (1 out of 3
587 experiments). Relative phosphorylation of (e) AKT (ser473) and (f) proteins in the MAPK
588 signaling pathway (both assayed on the same samples; n=4 experiments). Gene expression

589 from M0 and M1 macrophages incubated with or without 1 $\mu\text{g/ml}$ insulin: (g) *Slc2a1*
590 (encoding GLUT1) and (h) *Hk2* (encoding hexokinase 2); data are expressed as fold change
591 from untreated naive controls (n=9, 3 experiments). (i) Extracellular acidification rate (ECAR;
592 mpH/min) from polarized macrophages incubated for 2 hours in the presence or absence of
593 1 $\mu\text{g/ml}$ insulin. (n=12 or 15; 3 experiments). (j) ECAR measurements from M1 polarized
594 macrophages acutely treated with or without 1 $\mu\text{g/ml}$ insulin and 10 μM LY294002 or 10 μM
595 U0126 (vertical line indicates treatment start, n=9; 3 experiments) (k) Glucose uptake in
596 naive macrophages (control; n=21; 3 experiments) or incubated for 3 hours with 1 $\mu\text{g/ml}$
597 insulin alone (n=28; 3 experiments) or in combination with 1 ng/ml IL-1 β (n=15; 3
598 experiments). * $P < 0.05$, ** $P < 0.01$, *** $P < 0.001$, **** $P < 0.0001$. Statistical significance (P)
599 was determined by ANOVA and in (b, g) by Student's t test. All error bars denote s.e.m.

600

601 **Figure 6**

602 **Insulin stimulates IL-1 β secretion of macrophages.**

603 (a) Two-hour IL-1 β secretion from 2-hour polarized macrophages isolated from WT or *Nlrp3*^{-/-}
604 mice incubated with or without 1 $\mu\text{g/ml}$ insulin. (b-d) Two-hour IL-1 β protein release from
605 2-hour polarized M1 macrophages with or without 1 $\mu\text{g/ml}$ insulin and in combination with
606 or without (b) 10 μM LY294002 or 20 μM rapamycin (n=9-12; 3 experiments), (c) 50 μM
607 fasentin (n=14, 3 experiments), and (d) 2-deoxyglucose (2DG) or mitoTEMPO (n=6, 3
608 experiments); data are presented as fold stimulation from non-treated cells. (e) IL-1Ra and
609 (f) IL-1 β protein release from 16-hour polarized macrophages incubated for 12 hours with or
610 without 1 $\mu\text{g/ml}$ insulin (n=9, 3 experiments). (g) Circulating IL-1 β levels in mice treated with
611 or without 1 unit/kg insulin (15 minutes post injection; n=10). * $P < 0.05$, ** $P < 0.01$, *** $P <$
612 0.001. Statistical significance (P) was determined by ANOVA. All error bars denote s.e.m.

613

614

615 **Figure 7**

616 **IL-1 β shifts glucose uptake to immune cells.**

617 *In vitro* glucose uptake in (a) macrophages incubated with or without 1 ng/ml IL-1 β for 2
618 hours (n=15 and 11, respectively; 3 experiments) and, in (b) macrophages incubated with or
619 without 1 μ g /ml IL-1Ra for 3 hours (n=10 and 14, respectively; 3 experiments). (c-g) WT
620 mice were injected i.p. with either saline or 1 μ g/kg IL-1 β or 1 μ g/kg insulin (n=4 per group)
621 18 minutes prior to an injection of 10 μ Ci 3 H labeled 2DG. Mice were sacrificed 48 minutes
622 after the first injection followed by assessment of glucose uptake in spleen (c), circulating
623 leukocytes (d), visceral adipose tissue (epididymal fat pads; e), adipocytes isolated from
624 epididymal fat pads (f) and muscle (g). (h) Number of peritoneal cells and (i) *ex vivo* glucose
625 uptake in macrophages from mice injected once a day for 3 days with 35 μ g/kg IL-1 β (n=5
626 per group). (j) *Ex vivo* glucose uptake in peritoneal macrophages from mice acutely injected
627 with saline or 10 mg/kg IL-1Ra. (k) Circulating blood glucose and insulin levels during an
628 intra-peritoneal glucose tolerance test after treatment with 1 μ g/kg IL-1 β in macrophage-
629 depleted *Rag2*^{-/-} mice using an injection of 10 ml/kg clodronate or PBS liposomes (PBS; n=13,
630 clodronate; n=8). **P* < 0.05, ***P* < 0.01, ****P* < 0.001, *****P* < 0.0001. Statistical significance
631 (*P*) was determined by Student's t test and in (c-g by ANOVA). All error bars denote s.e.m.

632

633 **Online methods**

634

635 **Human pancreatic islets**

636 Human islets were isolated in the islet transplantation centres of Lille and Geneva from
637 pancreata of cadaver organ donors in accordance with the local Institutional Ethical
638 Committee. They were obtained via the “islet for research distribution program” through
639 the European Consortium for Islet Transplantation, under the supervision of the Juvenile
640 Diabetes Research Foundation (31-2008-416). Islets were cultured in CMRL-1066 medium
641 containing 5 mmol/l glucose, 100 units/ml penicillin, 100 µg/ml streptomycin, 2 mM
642 Glutamax and 10 % FCS (Invitrogen) on extracellular matrix-coated 24-well plates (Novamed
643 Ltd.) in humid environment containing 5 % CO₂.

644

645 **Mouse pancreatic islets**

646 To isolate mouse islets, pancreata were perfused through the sphincter of oddi with a
647 collagenase solution (1.4 gr/l; collagenase type 4 Worthington) and digested in the same
648 solution at 37°C, followed by sequential filtration through 500 µm and 70 µm cell strainers
649 (BD). Islets were handpicked and cultured on extracellular matrix-coated 24-well plates
650 (Novamed Ltd.) in RPMI-1640 (GIBCO) containing 11.1 mM glucose, 100 units/ml penicillin,
651 100 µg/ml streptomycin, 2 mM Glutamax, 50 µg/ml gentamycin, 10 µg/ml Fungison and 10
652 % FCS. Islets were either collected directly for RNA isolation extraction or cultured for 36
653 hours on extracellular matrix-coated 24-well plates for subsequent glucose-stimulated
654 insulin secretion experiments.

655

656 **Glucose-stimulated insulin secretion assay in islets and ENDOC cells**

657 For glucose-stimulated insulin secretion experiments, islets or the human β-cell line ENDOC
658 cells (kindly provided by R. Sharfmann⁵¹) were cultured for 2 days and pre-incubated for 30

659 minutes in modified Krebs-Ringer bicarbonate buffer (KRB; 115 mM NaCl, 4.7 mM KCl, 2.6
660 mM $\text{CaCl}_2 \cdot 2\text{H}_2\text{O}$, 1.2 mM KH_2PO_4 , 1.2 mM $\text{MgSO}_4 \cdot 2\text{H}_2\text{O}$, 10 mM HEPES, 0.5 % bovine serum
661 albumin, pH 7.4) containing 2.8 mM glucose. KRB was then replaced by KRB with 2.8 mM
662 glucose and collected after 1 hour to determine the basal insulin release. IL-1 β was added at
663 the indicated concentrations for the last 30 minutes of the 1-hour period of the basal insulin
664 release (priming). This was followed by 1 hour in KRB with 16.7 mM glucose to determine
665 the stimulated insulin release. The stimulatory index was defined as the ratio of insulin
666 secretion at 16.7 mM to 2.8 mM glucose/hour and expressed as percentage of untreated
667 control.

668

669 **Animal experiments**

670 All animal experiments were performed in mice on a C57BL/6N background unless otherwise
671 specified. Normal mice were obtained from Charles River. For the diet induced obesity (DIO)
672 experiments, 4 week old mice were fed a high fat diet (D12331, Research Diets; containing
673 58, 26 and 16 % calories from fat, carbohydrate and protein, respectively) for 20-25 weeks.
674 Leptin receptor deficient (db/db) mice were obtained from Jackson laboratories at the age
675 of 4 weeks and housed until the age of 16 weeks. *Irak4*^{-/-} mice on a Balb/c background were
676 kindly provided by Amgen. *IL1b*^{-/-} mice mouse strains on a C57BL/6N background produced
677 either by gene targeting⁵² or with Eucomm embryonal stem cells were used. To generate the
678 macrophage specific IL-1 β knock-out mouse (*Il1b*^{fl/fl}*Lyz2-Cre*^{+/+}) chimeric mice were produced
679 from ES cells containing a modified *Il1b* allele, which contains loxP sites flanking exons 4 and
680 5 and a frt-LacZ-loxP-neo-Frt cassette introduced between exon 3 and 4 (Eucomm clone
681 HEPD0840_C04). Chimeric mice were then crossed with C57BL6/N mice and the offspring
682 with germ line transmission of the recombined allele were crossed with Flp deleter mice⁵³
683 on Bl6/N background to excise the FRT flanked lacZ neo cassette and to obtain the *Il1b*^{fl/fl}
684 mouse. These mice were next crossed with *Lyz2-Cre* mice⁵⁴, that were previously

685 backcrossed to a C57BL6/N background. As littermate control mice we used the cre
686 recombinase negative *Il1b^{fl/fl}Lyz2-Cre^{-/-}* mice, and as myeloid cells specific *Il1b^{-/-}* knock-out
687 mice the *Il1b^{fl/fl}Lyz2-Cre^{+/-}* mice (Supplementary Fig. 1c). *Nlrp3^{-/-}* mice were generated as
688 described previously⁵⁵. *Rag2^{-/-}* mice were bred in house. *Il1r1^{-/-}* mice and immunodeficient
689 female swiss nude were obtained from Charles River laboratories. *Glpr^{-/-}/Grp^{-/-}* mice were
690 generated as described⁵⁶.

691

692 All animal experiments were conducted according to the Swiss Veterinary Law and
693 Institutional Guidelines and were approved by the Swiss Authorities. All animals were
694 housed in a temperature-controlled room with a 12 h light – 12 h dark cycle and had free
695 access to food and water.

696

697 All metabolic experiments using transgenic mice were performed with wild-type littermates
698 as controls. The mice were between 12 and 29 weeks of age. Mice that did not gain weight
699 in diet-induced obesity experiments were excluded. All experiments were performed at least
700 twice with weight-matched mice and with at least a total of 4 animals per group. For drug
701 applications (apart from antibiotics treated mice that can receive commensal bacteria from
702 non treated controls) each cage included mice receiving all treatments in order to avoid cage
703 dependent differences.

704

705 ***In vivo* treatment administration**

706 Recombinant mouse IL-1 β (R&D) was injected i.p. at the indicated time and dose.
707 IL-1Ra (Anakinra; 10 mg/kg body weight) was injected i.p. 3 hours prior to intervention. 2-
708 deoxyglucose (1 g per kg body weight) was injected i.p. 1 hour prior to refeeding.
709 Canagliflozin (100 mg per kg body weight) or placebo control were homogenised and orally

710 administered 1 hour prior to refeeding. LPS (InvivoGen; 1 mg/kg body weight) was injected
711 i.p. at the indicated time.

712

713 **Glucose tolerance tests (GTTs)**

714 For glucose tolerance testing, mice were fasted for 6 hours starting in the morning and 2 g
715 glucose per kg body weight was injected i.p. Blood glucose was measured using a
716 glucometer (Freestyle; Abbott Diabetes Care Inc.).

717

718 **Urine glucose levels**

719 Glycosuria was assessed according to manufacturer's instructions (Accu Check Diabur test
720 strips, Roche)

721

722 **Fasting and refeeding experiments**

723 Before blood collection, fasted mice were provided free access to water but not to food for
724 12 hours. Refed mice were treated in the same manner as the fasted mice; however, prior to
725 blood collection, refed mice had access to food for 2 hours. In experiments done with
726 antibiotics or with IL-1Ra injection or with *IL1b*^{-/-} mice and littermate wild-type mice, blood
727 was collected immediately before refeeding (time 0) and 2 hours after feeding. To avoid
728 potential confounding effects due to circadian-mediated fluctuation in circulating IL-1β
729 levels all experiments were performed at the same time of the day (between 8 to 10 am).

730

731 **Glucose clamp studies**

732 Glucose clamp studies were performed in freely moving mice as previously described⁵⁷.
733 Steady state glucose infusion rate was calculated once glucose infusion reached a constant
734 rate with blood glucose levels at 5 mmol/l (70-80 minutes after the start of insulin infusion).
735 Thereafter, blood glucose concentration was kept constant at 5 mmol/l for 15-20 minutes

736 and glucose infusion rate was calculated. Glucose disposal rate, and hepatic glucose
737 production were calculated as previously described⁵⁷.

738

739 **Antibiotics treatment**

740 One week before fasting-refeeding experiment, 1 g/l antibiotic concoction consisting of
741 vancomycin 10 mg/ml, neomycin 20 mg/ml, metronidazol 20 mg/ml (all purchased from
742 Sigma), was administered by gavage every 12 hours. Gavage volume of 5 ml/kg body weight
743 was delivered with a stainless steel tube. Fresh antibiotics concoction was mixed every day.

744

745 **Streptozotocin induced β -cell death and Islet transplantation.**

746 Streptozotocin (Sigma) was dissolved in citrate buffer (pH 4.5) and was i.p. injected to
747 immunodeficient nude mice at 240 mg/kg. Only hyperglycemic mice (i.e. blood glucose >
748 14mM) were subjected to transplantation with 500 wild-type or *Il1r1*^{-/-} mouse islets, under
749 the kidney capsule as described in⁵⁸.

750

751 **Macrophage ablation**

752 Clodronate or PBS liposomes (ordered from ClodronateLiposomes.org) were injected i.p.
753 (100 μ l per 10 grams bodyweight) 3 days before the start of the assays. Mice were sacrificed
754 at the end of the procedure. To verify macrophage depletion, peritoneal cells were isolated
755 as described above and analyzed by FACS as described below. Macrophages were defined as
756 CD11b⁺ F4/80⁺ double positive cells.

757

758 **Primary cell isolation and culture**

759 Cells were isolated from male C57BL/6 mice following euthanasia in a CO₂ chamber. To
760 obtain circulating leukocytes, the heart was punctured and the collected blood was
761 incubated briefly with red blood cells lysis buffer (154mM NH₄Cl, 10mM KHCO₃, 0.1mM

EDTA). To isolate macrophages, the peritoneum was infused with PBS containing 1% FBS and the lavage was filtered through 70 μ m cell strainer (BD). Kupffer cells were isolated from the liver perfused with 3mL collagenase through the ductal vein followed by a 30 minute incubation step and two centrifugation steps: 50 x g for 3 minutes at 4 °C, collection of the upper phase and 350 x g for 5 minutes at 4°C. Intestinal macrophages were isolated after removal of the intestinal Peyer patches, cut in pieces and washed twice (20 min shaking in PBS, 5mM EDTA), followed by 30min incubation in collagenase type 4 (1.4 g/l). Cells from omental and epididymal fat pads were isolated after shaking with collagenase type 4 (1.4 g/l) for 30 min at 37°C. Spleens were pushed through a 70 μ m cell strainer and red cells were lysed using lysis buffer (154mM NH₄Cl, 10mM KHCO₃, 0.1mM EDTA). For islet resident macrophages, handpicked pancreatic islets were dissociated by accutase (Biolegend, 50%, 2 minutes, 37 degrees) and washed. All cells were filtered through a 70 μ m cell strainer washed and resuspended in FACS buffer (PBS 0.5% BSA and 5mM EDTA). For macrophage culture, cells were allowed to adhere for at least 4 hours in 48 or 96 well plates (TPP) and non-adherent cells were washed away, naive macrophages were used for glucose uptake assays or were polarized to M1 or M2 phenotypes as follows: 2 hours (serum free) or 16 hours treatment with LPS (100 ng/ml) + IFN γ (10 ng/ml) for M1 and IL-13 (10 ng/ml) + IL-4 (10 ng/ml) for M2 polarization, followed by 2 or 12 hours, with or without 1 μ g/ml insulin in the presence or absence of fasentin (50 μ M; Sigma), 2-deoxyglucose (2DG; 10mM; Sigma), mito-TEMPO (100 μ M; Sigma), LY294002 (10 μ M; Sigma), U0126 (10 μ M; Sigma), rapamycin (20 μ M; Sigma) or followed by a 30 minute incubation with ATP (5mM; Sigma). Supernatants were collected, centrifuged (at 4°C, 2000 x g for 5 minutes) and stored at -80°C and cells were either harvested for RNA extraction (see RNA extraction and qPCR) or assayed by flow cytometer for cell survival using Annexin V apoptosis detection kit (eBioscience).

786

787 **RNA extraction and qPCR**

788 Total RNA was extracted using the Nucleo Spin RNA II Kit (Machery Nagel) or using RNeasy
 789 Lipid Tissue (QIAGEN). RNA concentrations were normalized and cDNA was prepared with
 790 random hexamers (Microsynth) and Superscript II (Invitrogen) according to the instructions
 791 of the supplier. RNA expression was determined with TaqMan assays and the real time PCR
 792 system 7500 (Applied Biosystems). The following TaqMan assays were used:
 793 Mouse: *Gadph*: Mm99999915_g1, *Actb*: Mm00607939_s1, *Slc2a1* (encoding GLUT1):
 794 Mm00441480_m1. *Il1b*: Mm0043228_m1, *InsR*: Mm01211875_m1, *Cxcl1*:
 795 Mm04207460_m1, *Hk2*: Mm00443395_m1, *Il1a*: Mm00439621_m1, *Il1r1*:
 796 Mm00434237_m1, *Ccl2*: Mm00441242_m1, *Tnf*: Mm00443258_m1, *Il6*: Mm004461920_m1.
 797 Data were normalized with the geometrical mean of *Gadph* and *Actb* for macrophage mRNA
 798 and quantified using the comparative $2^{-\Delta\Delta CT}$ method.

799

800 **Protein and protein-phosphorylation measurement assays**

801 Insulin concentrations were determined using human insulin ultrasensitive ELISAs
 802 (Mercodia) or mouse/rat insulin kits (MesoScale Discovery). Mouse active GLP-1 was assayed
 803 using a MesoScale discovery kit. Protein phosphorylation was assayed using whole cell
 804 lysates (10 µg total protein) and MesoScale Discovery kinase phosphorylation assay kits (AKT
 805 signalling panel; K15177D and MAP kinase panel; K15101D) according to manufacturer's
 806 instructions. Mouse cytokine concentrations were assayed using the V-plex mouse IL-1β
 807 TNFα, IL-6, and CXCL1 kit from MesoScale Discovery with the following modifications: for
 808 circulating cytokine assay, after withdrawal, blood was incubated for 30 minutes at room
 809 temperature and sera were collected after 20 minutes of centrifugation (4°C, 2000 x g).
 810 Samples were incubated in the assay plate overnight at 4°C with gentle shaking. IL-1Ra was
 811 determined using ELISA assays (R&D).

812

813 **Glucose bio-distribution assay**

814 Male C57BL/6 mice were fasted for 3 hours in the morning, i.p. injected with IL-1 β (1 μ g/kg
815 body weight) or saline and 18 minutes later with 3 H labeled 2-deoxy glucose (10 μ Ci per
816 mouse, Perkin Elmer). After 30 minutes mice were sacrificed, quadriceps muscle, epididymal
817 adipose tissue and spleen were weighed, washed immediately in ice cold PBS and incubated
818 with lysis buffer (10% glycerol, 5% 2-mercaptoethanol, 2.3% SDS, 62.5mM Tris pH6.8, 6M
819 urea) followed by sonication. Leukocytes were isolated as described above, washed twice
820 with ice cold PBS, counted and lysed with 0.1% SDS. Triplicate samples were then measured
821 in a beta counter. Data are presented for organs as percentage beta counts per minute per
822 mg tissue and as beta counts per cell for Leukocytes. In experiments with refed mice,
823 fluorescent 2-deoxyglucose (2NBDG 500nmole per mouse; Invitrogen) was i.p. injected
824 immediately after a refeeding window. Mice were sacrificed 1 hour later, peritoneal cells
825 were harvested and analyzed by flow cytometer (BD Acurri).

826

827 ***In vitro* glucose uptake assay**

828 For *in vitro* treatment, macrophages were pre-incubated for 2 hours with KRB containing 1
829 mM glucose (as described in GSIS section) with or without the indicated treatment. To
830 determine glucose uptake, macrophages were then incubated for 30 minutes with 0.4 nCi 3 H
831 labeled 2-deoxy glucose (Perkin Elmer), washed twice with ice cold PBS, lysed with 0.1 % SDS
832 and transferred into scintillation fluid. 3 H labeled 2-deoxy glucose uptake was measured in a
833 beta counter.

834

835 **Immunoblotting**

836 We separated proteins (8-12 μ g) in 4-12 % NuPAGE gels (Invitrogen), blotted them onto
837 nitrocellulose membranes (Bio-Rad) and incubated them with antibodies against total AKT
838 (pan AKT; #4691), pAKT (s473; #9271) and Insulin receptor β (4B8; #3025.) All antibodies

839 were purchased from Cell Signaling. Blots were analyzed using image lab 4.1 software (Bio-
840 Rad).

841

842 **Flow cytometry**

843 To obtain single cells, islets were dispersed with trypsin (Invitrogen) for 6 minutes at 37°C,
844 washed with PBS, centrifuged at 300 x g, 5 minutes, 4°C and resuspended in FACS buffer
845 (PBS with 0.5% BSA and 2 mM EDTA). After 15 minutes incubation with an Fc blocker (Anti-
846 mouse CD16/CD32; eBioscience 14-0161) peritoneal cells or single islet cells were stained
847 with the appropriate antibodies for 30 minutes at 4°C in the dark. To verify the effect of the
848 clodronate depletion, cells from Rag^{-/-} mice were stained with anti F4/80 (clone BM8) and
849 anti CD11b (clone M1/70). To determine the peritoneal cell composition, cells were stained
850 with anti CD3e (clone 145-2C11), anti GR-1 (clone RB6-8C5), anti CD11b (clone M1/70), anti
851 F4/80- (clone BM8), anti CD19 (clone RA3-6B2) and anti Siglec-F-APC (clone E50-2440).
852 Single cells from adipose tissue, islets, Liver, small intestine, and colon were stained with
853 CD45 (clone 30-F11) for immune cells (antibodies were purchased from eBioscience, Siglec-F
854 was purchased from BD Pharmingen). For additional intra-cellular Insulin receptor intensity
855 in tissue resident macrophages, cells were also incubated with intracellular fixation buffer
856 (eBioscience) following incubation with permeabilization buffer (eBioscience) according to
857 manufacturer's instructions. Anti InsR β (Cell Signaling; 3025S) was added following
858 secondary conjugated donkey anti rabbit antibody (Invitrogen). Stained cells were washed
859 twice with FACS buffer prior to FACS acquisition. Cells were analyzed with an Accuri C6 flow
860 cytometer or LSR-Fortessa (BD Bioscience). Dispersed islet cells were analyzed and sorted
861 with a FACS ARIA III cell sorter (BD Biosciences) using FACS Diva software (BD Biosciences).
862 All samples were stained with appropriate isotype control antibodies; viability staining was
863 done using 7-AAD (Sigma) or DAPI (Biolegend). Macrophages were defined as CD11b⁺ F4/80⁺
864 double positive cells. Data were analyzed using Flow Jo 9.4 software (Tree Star).

865

866 **Extracellular acidification measurements**

867 An XF24 or an XF96 Extracellular Flux analyzer (Seahorse Biosciences) was used to
868 determine the bioenergetic profile of FACS sorted macrophages (F4/80 and CD11b double
869 positive peritoneal cells). Cells were plated at a density of 500'000 or 300'000 cells per well
870 in XF24 or XF96 plate accordingly, incubated for 4 hours and washed before being
871 stimulated with LPS (100 ng/ml) + IFN γ (10 ng/ml) or IL-4\IL-13 (10 ng/ml) for the indicated
872 times. Insulin was injected or added to the media (1 μ g/ml end concentration) for the
873 indicated time. Prior to the assay, cells were incubated in unbuffered RPMI (Seahorse
874 Biosciences) containing 11.1 mM glucose for 1 hour. Then extracellular acidification rate
875 were assessed during 2 minutes. Basal measurements were followed by measurements
876 upon injection of the following agents: Glucose (26.8 mM), oligomycin (1 μ M),
877 carbonilcyanide p-triflouromethoxyphenylhydrazone (FCCP) (2 μ M), rotenone (1 μ M), and 2-
878 deoxyglucose (2DG; 10mM). To activate cells with insulin during Seahorse measurments cells
879 were incubated in unbuffered RPMI containing 5mM glucose for 1 hour, then extracellular
880 acidification rate were assessed during 2 minutes for 6 basal measurements followed by
881 injections of inhibitors (LY294002, 10 μ M; U0126, 10 μ M) or DMSO as control and insulin (1
882 μ g/ml). Oligomycin, FCCP, and rotenone were purchased from Sigma.

883

884 **Immunofluorescence staining**

885 Pancreata were fixed overnight in 4% paraformaldehyde at 4°C, followed by paraffin
886 embedding. Sections were deparaffinized, re-hydrated and incubated 1 hour at room
887 temperature with guinea pig anti-insulin antibody (Dako; A0564), followed by detection with
888 a fluorescein-conjugated donkey anti-guinea pig antibody (Dako). Subsequently, the sections
889 were labeled for IL-1R1 with goat anti IL-1-R1 antibody (R&D; AF771), followed by detection
890 with a fluorescein-conjugated donkey anti-goat antibody (Invitrogen).

891

892 **Statistics**

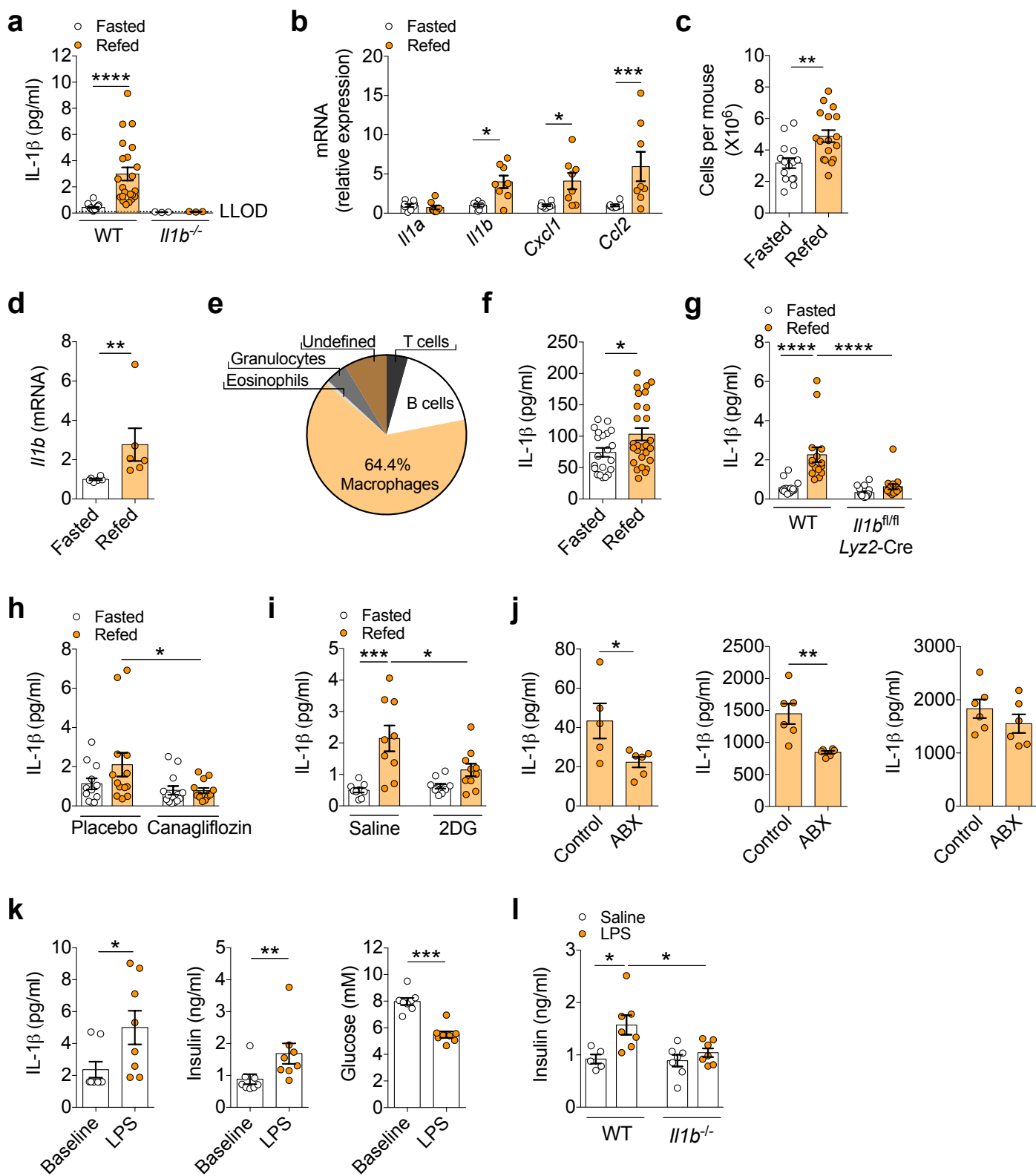
893 Appropriate statistical tests were performed where required. Comparisons between groups
894 were performed using unpaired, two-sided *t*-test for normally distributed data. For grouped
895 comparisons, one-way ANOVA or two-way ANOVA followed by Sidak's multiple comparisons
896 analysis were used where appropriate. Statistically significant outliers were assessed using
897 ROUT's test ($\alpha = 1\%$) and were excluded from analysis. Data analysis was performed using
898 GraphPad Prism v7.0a Software. Excluding diet induced obesity experiments, all animal
899 studies were performed on weight matched mice. There was no other prior randomization
900 or blinding. Data are expressed as means \pm s.e.m. and statistical significance is denoted as * P
901 < 0.05 , ** $P < 0.01$, *** $P < 0.001$ and, **** $P < 0.0001$. *n* numbers indicate biological
902 replicates for *in vitro* experiments or number of mice for *in vivo* experiments.

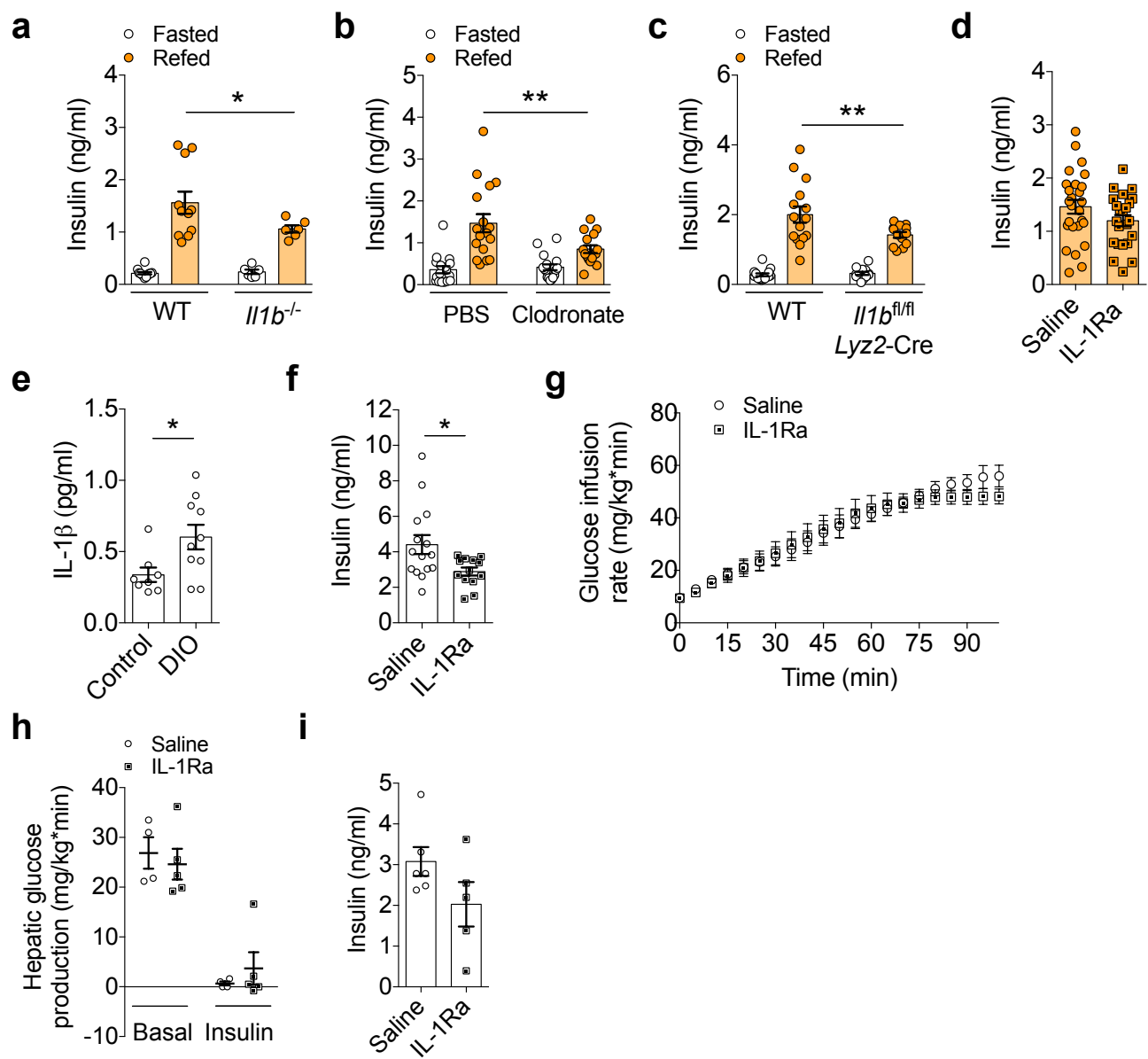
903

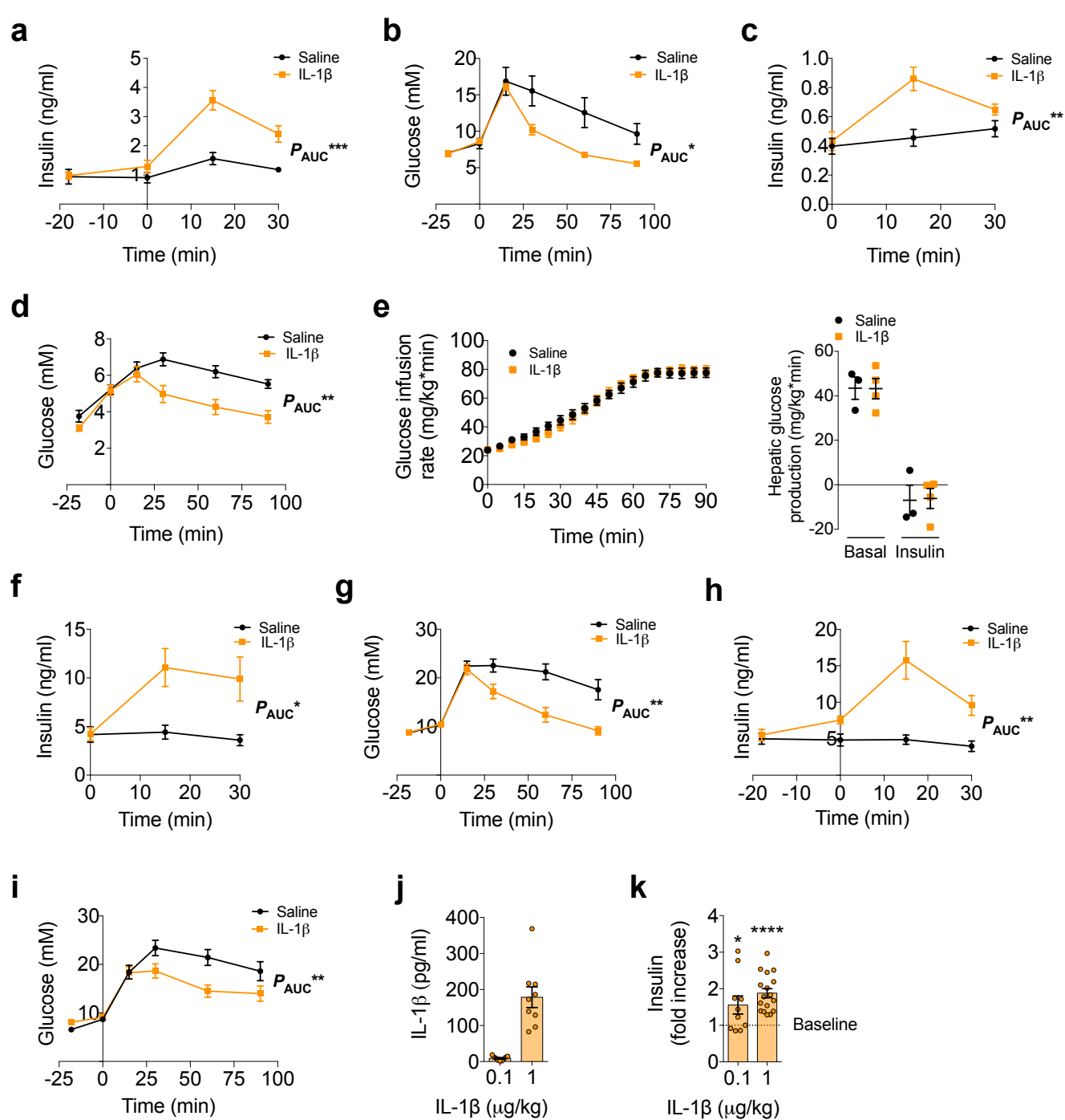
904 **Method-only references**

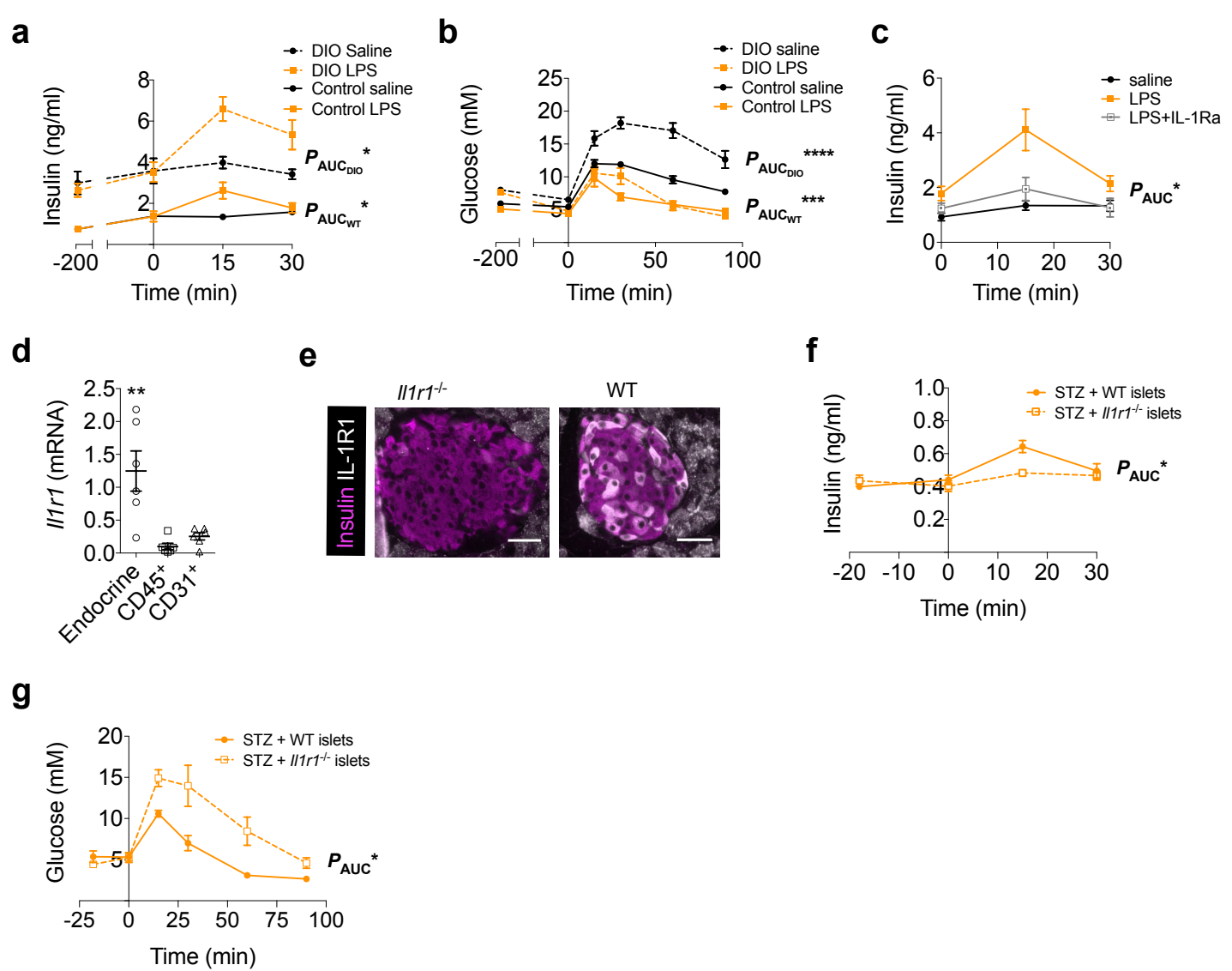
- 905 51. Ravassard, P., *et al.* A genetically engineered human pancreatic beta cell line
906 exhibiting glucose-inducible insulin secretion. *The Journal of clinical investigation*
907 **121**, 3589-3597 (2011).
- 908 52. Horai, R., *et al.* Production of mice deficient in genes for interleukin (IL)-1alpha, IL-
909 1beta, IL-1alpha/beta, and IL-1 receptor antagonist shows that IL-1beta is crucial in
910 turpentine-induced fever development and glucocorticoid secretion. *The Journal of*
911 *experimental medicine* **187**, 1463-1475 (1998).
- 912 53. Farley, F.W., Soriano, P., Steffen, L.S. & Dymecki, S.M. Widespread recombinase
913 expression using FLP_{er} (flipper) mice. *Genesis* **28**, 106-110 (2000).
- 914 54. Clausen, B.E., Burkhardt, C., Reith, W., Renkawitz, R. & Forster, I. Conditional gene
915 targeting in macrophages and granulocytes using LysMcre mice. *Transgenic research*
916 **8**, 265-277 (1999).

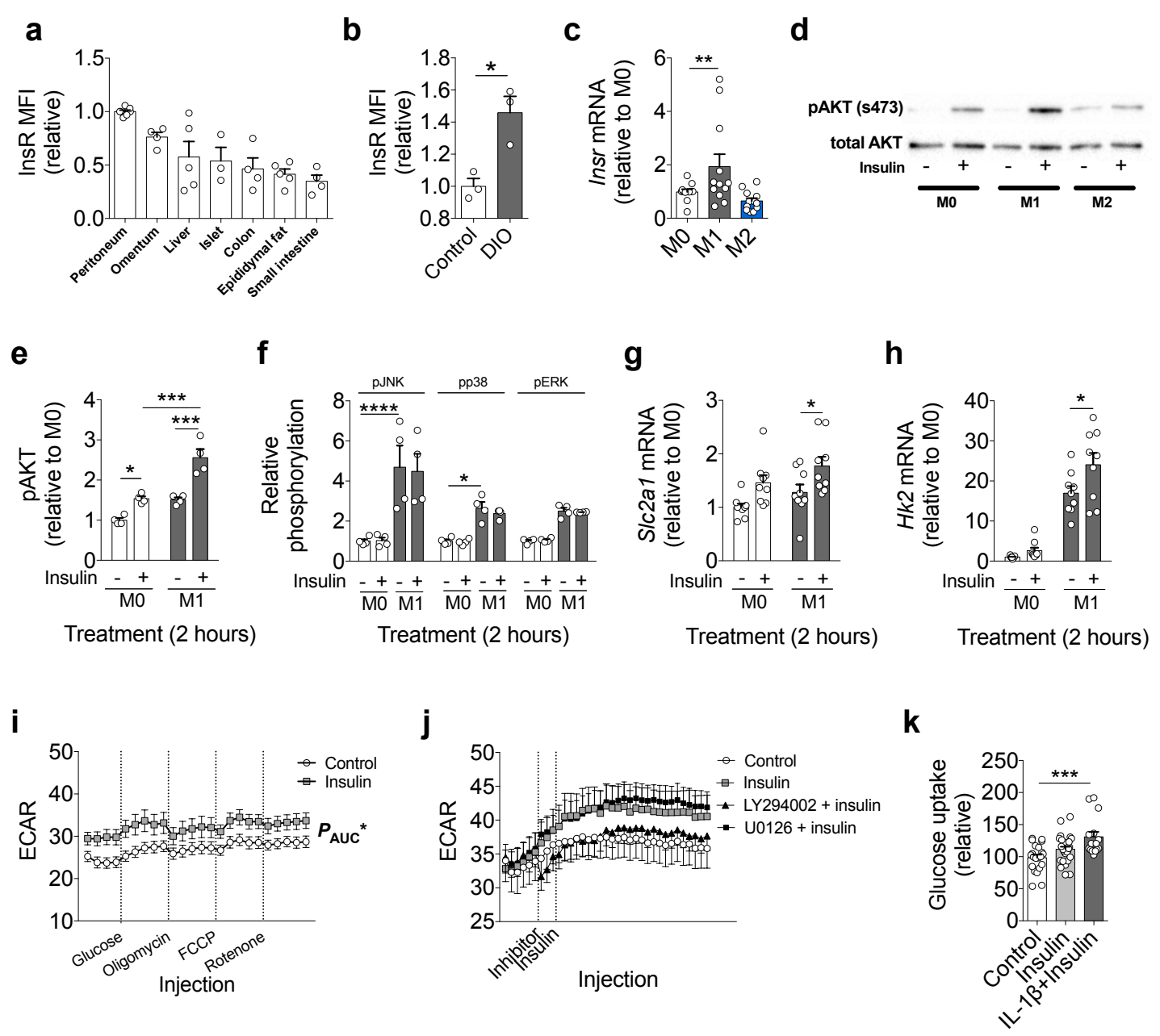
- 917 55. Martinon, F., Petrilli, V., Mayor, A., Tardivel, A. & Tschopp, J. Gout-associated uric
918 acid crystals activate the NALP3 inflammasome. *Nature* **440**, 237-241 (2006).
- 919 56. Preitner, F., *et al.* Gluco-incretins control insulin secretion at multiple levels as
920 revealed in mice lacking GLP-1 and GIP receptors. *The Journal of clinical*
921 *investigation* **113**, 635-645 (2004).
- 922 57. Wueest, S., *et al.* Fas (CD95) expression in myeloid cells promotes obesity-induced
923 muscle insulin resistance. *EMBO molecular medicine* **6**, 43-56 (2014).
- 924 58. Caiazzo, R., *et al.* Quantitative in vivo islet potency assay in normoglycemic nude
925 mice correlates with primary graft function after clinical transplantation.
926 *Transplantation* **86**, 360-363 (2008).
- 927
- 928

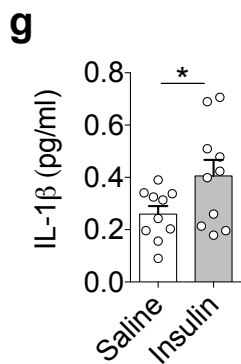
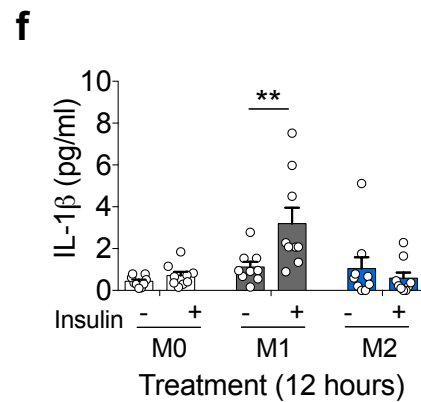
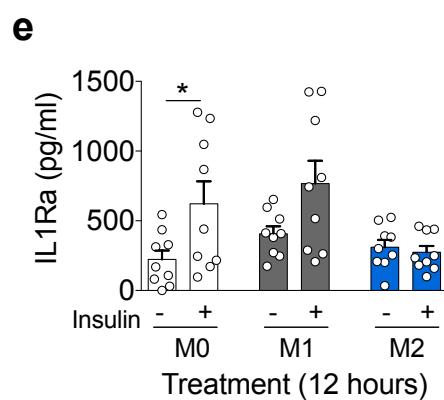
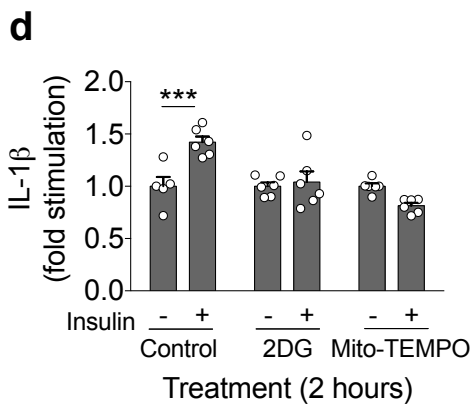
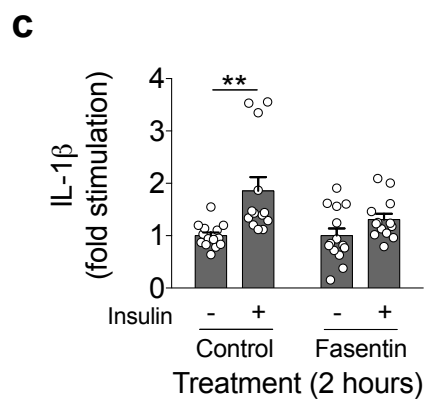
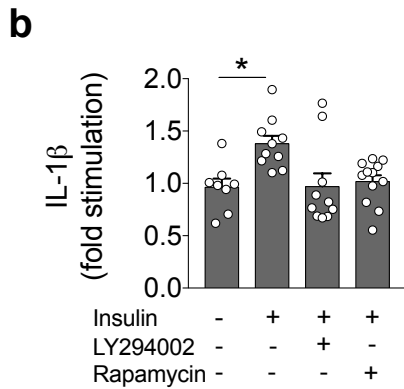
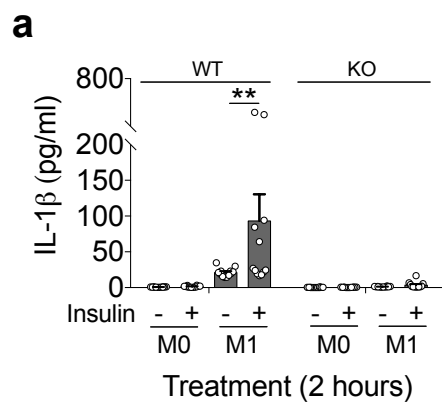


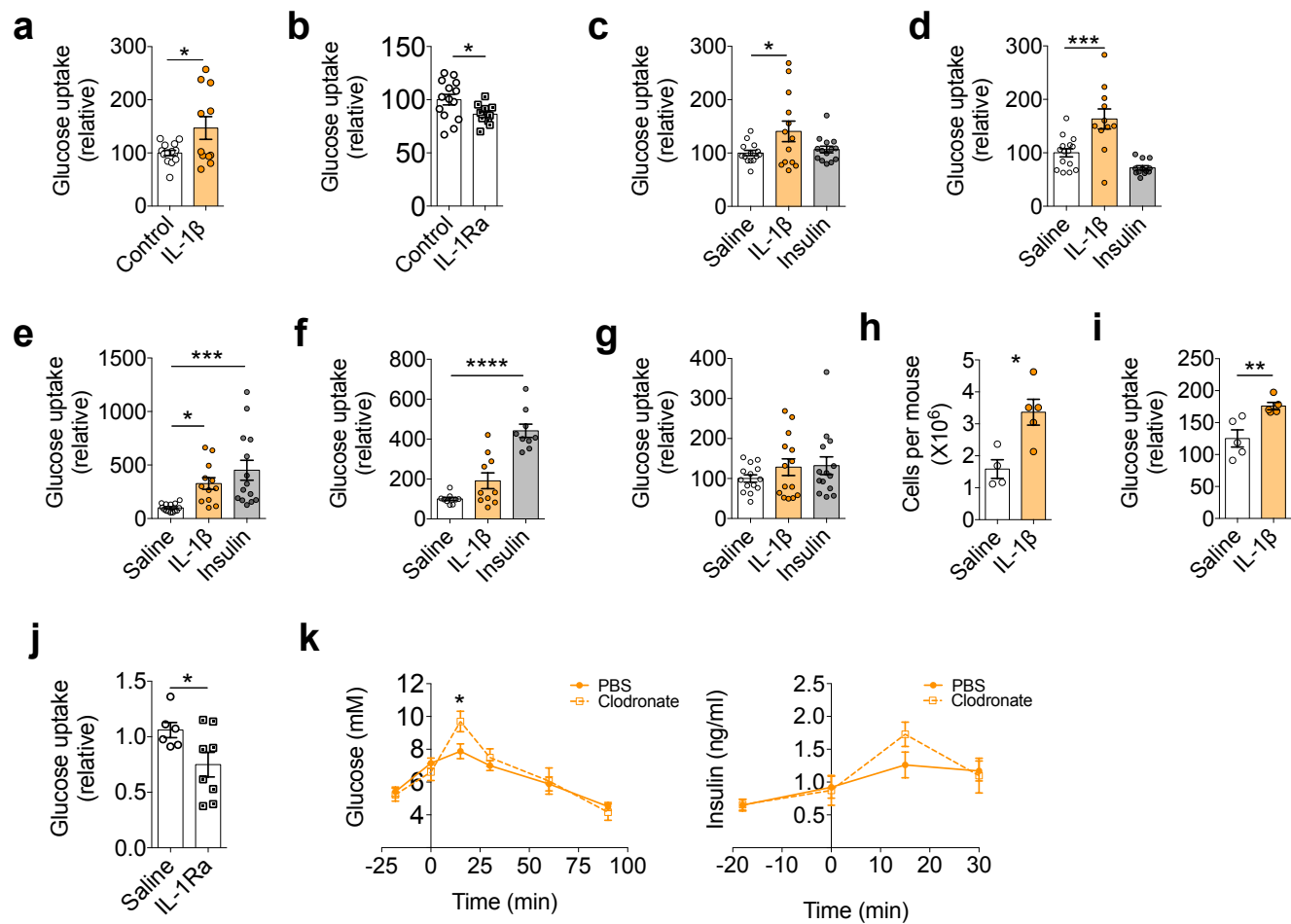


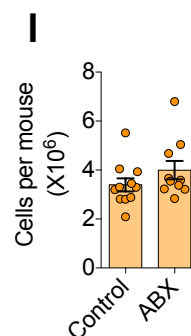
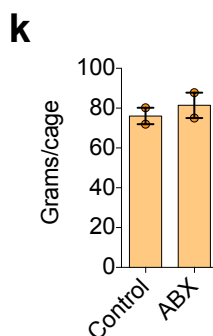
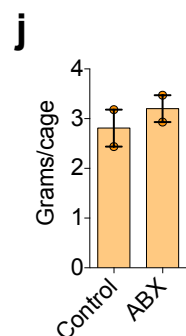
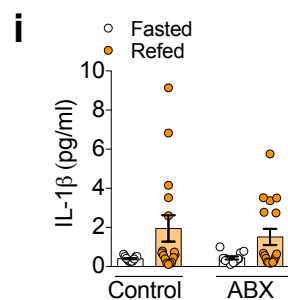
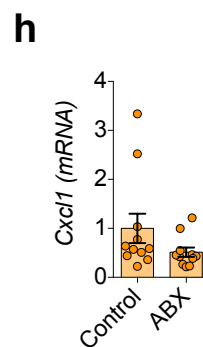
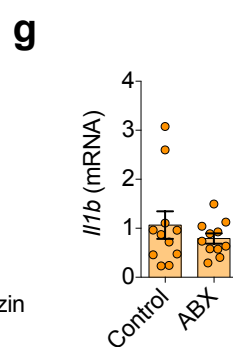
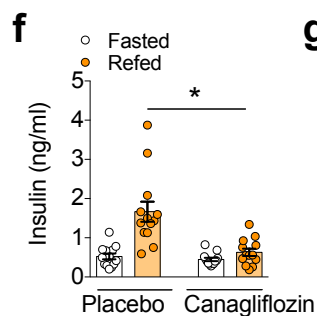
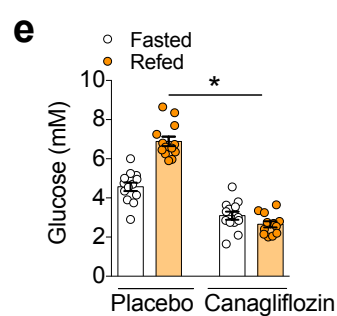
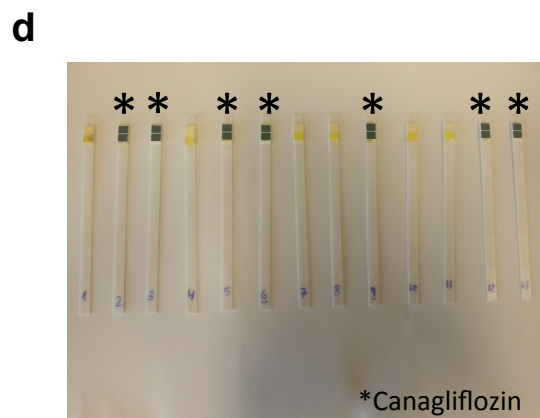
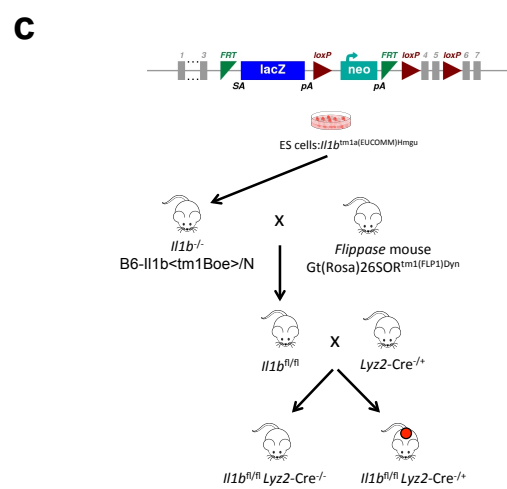
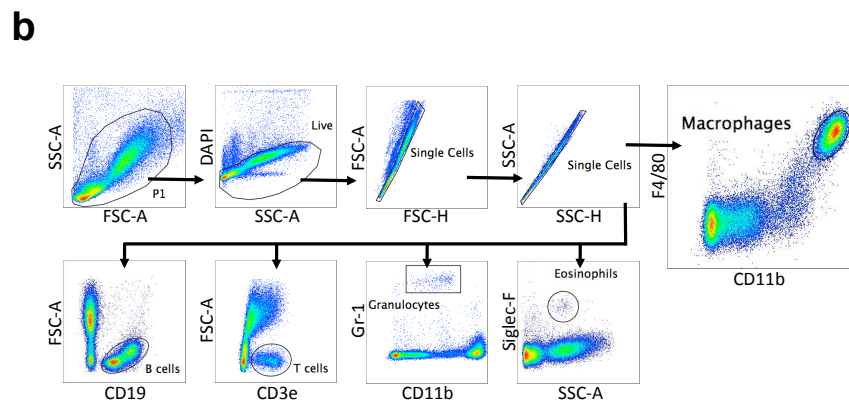
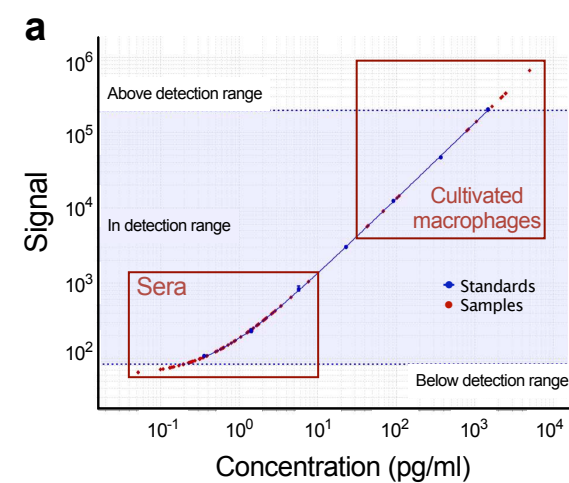


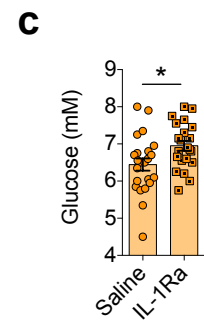
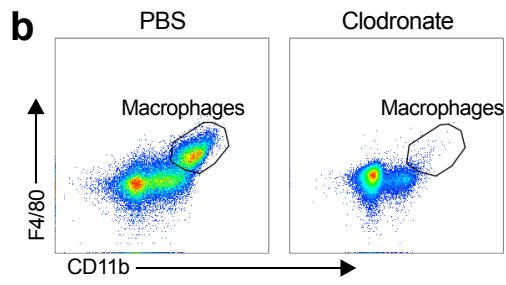
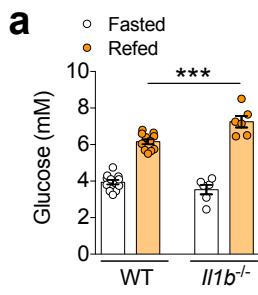


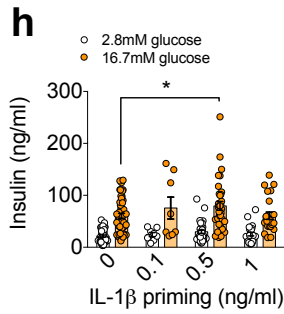
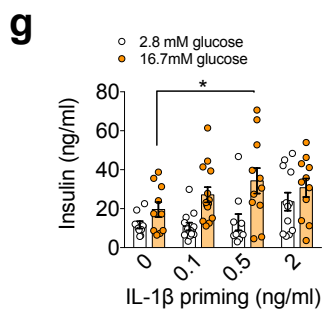
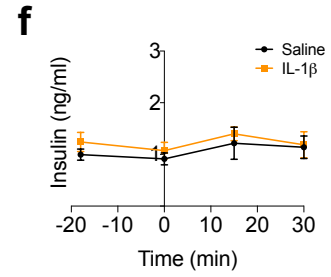
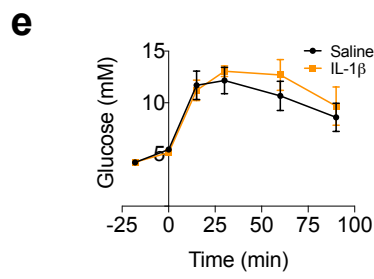
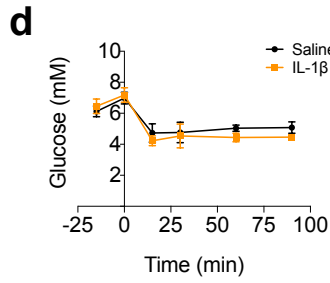
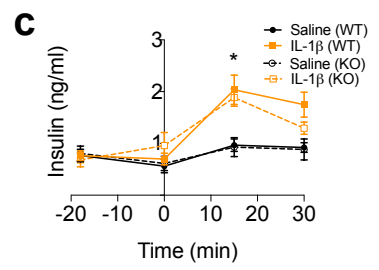
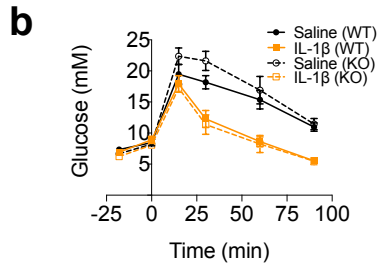
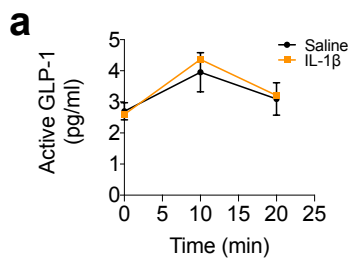


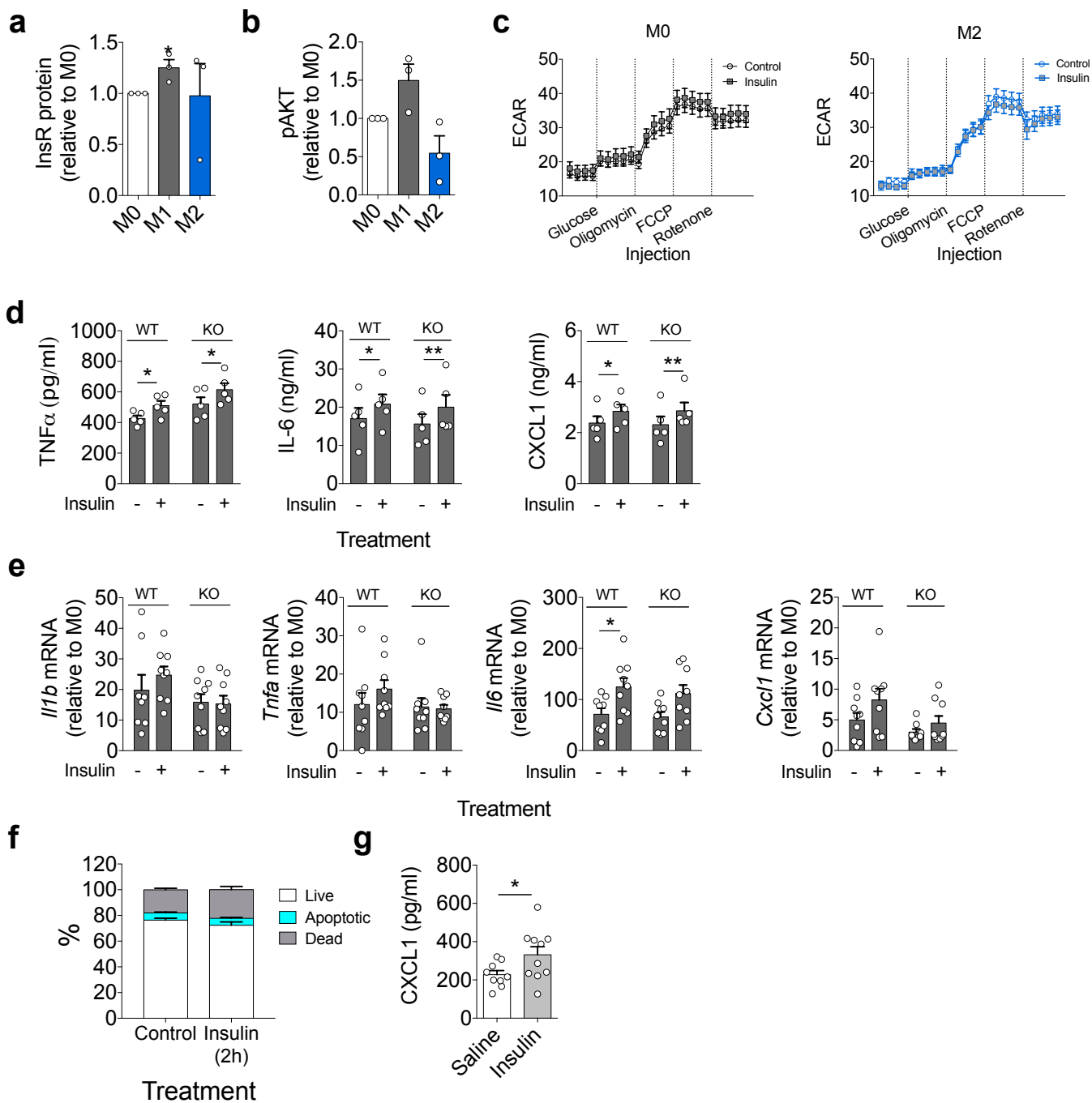


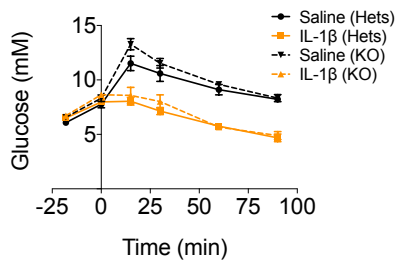










a**b**